

Tesis Doctoral

*Organic/Inorganic Hybrid Materials based
on Conducting Organic Polymers as
Electrodes for Energy Storage Devices*

Ana Karina Cuentas Gallegos

**Laboratorio de Química del Estado Sólido
Instituto de Ciencia de Materiales
Octubre 2003**

PEDRO GÓMEZ ROMERO, Scientific Researcher of the Materials Science
Institute of Barcelona (CSIC)

CERTIFIES:

That Ana Karina Cuentas Gallegos, with License in Chemical Sciences, has fulfill under his supervision the research carried out under the title “Hybrid materials based on organic conducting polymers and electroacative inorganic species for energy storage devises”, and that is contain in this memory.

And to be no doubt, signs the present certificate.

Bellaterra, at October 31st of 2003

Dr. Pedro Gómez Romero
ICMAB (CSIC)

Al Dr. Javier Rivas Ramos

Profesor emeritus del ÍTESM, Monterrey México

**The use of science without social conscience,
would lead us to the decay of human kind.**



Agradecimientos

Agradezco a mi madre y a mi abuela Esther por la ayuda económica durante los primeros dos años de ausencia de beca. A CONACYT y al Instituto de Ciencias de Materiales de Barcelona por la ayuda económica para la terminación de esta Tesis doctoral.

Quisiera agradecer a mi tutor, el Dr. Xavier Doménech por su amable colaboración.

A los doctores:

Dr. Jaume Casabó, Dr. Eduardo Ruiz Hitzky, Dr. Enric Brillas, Dr. Guy Campet, Dra. Nuria Ferrer, Dr. Francesc Teixidor y al Dr. Salvador Borrós por haber aceptado formar parte del tribunal del presente trabajo de Tesis.

Agradezco de una forma muy especial al Dr. Pedro Gómez Romero por haberme dado la confianza y libertad para desarrollar este trabajo, que ha contribuido mucho a mi formación como científica. Además, de haber ejercido como el director de este trabajo, le agradezco todos sus consejos que me han ayudado mucho para evolucionar como profesionalista y como persona. Por explicarme tan detalladamente conceptos que no comprendía, por las charlas que siempre he encontrado muy interesantes.

Quiero agradecer a Nieves Casañ por sus ideas que siempre me fueron muy útiles, y que me han abierto más los ojos en cuanto a todas las consideraciones que se deben de tener en cuenta durante la realización de un trabajo de investigación. Muchísimas gracias.

Quisiera agradecer a mi familia que siempre a estado al tanto de mí, a pesar de la distancia. A mi madre por apoyarme siempre creyendo en mí, y que a respetado mi estilo de vida. A mis hermanas Alejandra y Adriana por los buenos ratos que me han hecho pasar por teléfono y vía electrónica. A mi padre porque me ha hecho comprender que tan importante es mi vida profesional, me ha inculcado lo importante que es luchar por los ideales que uno tiene, y sobretodo el sentido de independencia y autosuficiencia. A mi Abuela Conchita por ser tan cariñosa y siempre estar ahí para mí, a mi abuela Esther por ser un ejemplo de prudencia, fuerza. Y toda mi familia tíos, tías, primas, primos, que me han apoyado mucho. Muchas gracias.

A mis compañeros de grupo que han hecho de mi estancia en Barcelona una buena experiencia: Eva, Gloria, Juan Antonio, David, Jordi, Gerard, Belén, y muy especialmente a la Montse. A la Dra. Rosa Palacín y la Dra. Amparo Fuertes por ayudarme con dudas que he tenido durante la realización de este trabajo. A Mónica Lira por su amistad, por sus consejos, por introducirme a este mundo de los materiales híbridos y las baterías en el laboratorio, y sobretodo por las platicas tan entretenidas que en algún momento hemos tenido. A todos los amigos que he hecho en el ICMAB, especialmente a Magda Moner (muy buena amiga) que me ha dado una perspectiva filosófica muy diferente y autentica de ver la vida.

A todas las personas que han contribuido indirectamente de una manera u otra para que estos dos años hayan sido divertidos. Entre ellas están mi gran amiga la diseñadora Ángeles Moreno que me ha enseñado a presentar mi trabajo de una manera más atractiva visualmente, a Mi gran amigo Bart que mediante las charlas existenciales que hemos tenido me ha enseñado a tomarme la vida con más filosofía. Muchas gracias!

Finalmente quiero agradecer de una manera muy especial a Francisco, por haber decidido en compartir su vida conmigo, por apoyarme en esta etapa de mi vida profesional que sabe que es súper importante para mí, y sobretodo que durante estos años de convivencia he aprendido muchísimo de él y de mi misma. Muchas Gracias!

Abbreviations

-----A-----

A1-----	Magnetic stirring with air bubbler
A2-----	Turbine mechanical stirring
A3-----	Turbo-propeller mechanical stirring
A4-----	Mechanical mixer
A5-----	A4 stirring but with stirring-rest intervals
AMnO ₄ -----	Permanganate anion
Ani-----	Aniline

-----B-----

BET-----	Brunauer, Emmett and Teller creators of surface area theory.
----------	--

-----C-----

CE-----	Counter electrode
COPs-----	Conducting organic polymers
CV-----	Cyclic voltammetry

-----D-----

DBP-----	Dybuthyl phtalate
DMC-----	Dymethyl carbonate

-----E-----

EC-----	Ethyl carbonate
EDTA-----	Ethylene diamine tetra acetic acid
ESCs-----	Electrochemical supercapacitors

-----F-----

FTIR-----	Infrared spectroscopy with Fourier transform
-----------	--

-----H-----

HCF-----	Ferrocyanide cluster/anion
----------	----------------------------

-----I-----

ICP-----	Induced coupled plasma
IO-----	Inorganic-organic hybrids

-----N-----

NMR-----	Nuclear magnetic resonance
----------	----------------------------

-----O-----

OI-----Organic-inorganic hybrids

-----P-----

PAni-----Polyaniline

PAni/HCF/V₂O₅-----Polyaniline, ferrocyanide, and vanadium pentoxide triple hybrid

PAni/MnO₂-----Polyaniline and manganese oxide hybrid

PAni/PMo12-----Polyaniline and phosphomolibdate hybrid

PAni/POMs-----Polyaniline and polyanions hybrids

PAni/PW12-----Polyaniline and phosphotungstate hybrid

PAni/SiW12-----Polyaniline and silicotungstate hybrid

PAni/V₂O₅-----Polyaniline and vanadium pentoxide hybrid

PAni/VOPO₄-----Polyaniline and vanadyl phosphate hybrid

PMca-----Sample obtained from aniline+MnSO₄·H₂O+KMnO₄+H₂SO₄

PMo12-----Phosphomolybdic acid

PMsa-----Sample obtained aniline+MnSO₄·H₂O+KMnO₄

POMs-----Polyoxometalates

ppm-----parts per million

PPy-----Polypyrrole

PPy/HCF/V₂O₅-----Polypyrrole, ferrocyanide, and vanadium pentoxide triple hybrid

PPy/MnO₂-----Polypyrrole and manganese oxide hybrid

PPy/VOPO₄-----Polypyrrole and vanadyl phosphate hybrid

PVDF-----Kinar flex (polyvinylidene fluoride)

PW12-----Phosphotungstic acid

Py-----Pyrrole

-----R-----

RE-----Reference electrode

-----S-----

SEM-----Scanning Electron Microscopy

SiW12-----Silicotungstic acid

-----T-----

TGA-----Thermogravimetric analyses

-----W-----

WE-----Working electrode

-----X-----

XRD-----Powder x-ray diffraction

Table of Contents

CHAPTER 1. *Introduction*

Abstract	1
1.1 Hybrid Materials	2
1.1.1. Classification	6
1.1.1.1. <i>Organic-Inorganic Materials (OI)</i>	7
1.1.1.2. <i>Nanoparticles dispersed in Conducting Organic Polymers: Hybrid Nanocomposites</i>	12
1.1.1.3. <i>Inorganic-Organic Materials (IO)</i>	12
1.2 Energy Storage Devices and Applications	14
1.2.1. Lithium Rechargeable Batteries	16
1.2.1.1. <i>Background</i>	16
1.2.1.2. <i>How does a Lithium Battery work?</i>	18
1.2.1.3. <i>Lithium Insertion Electrodes</i>	19
1.2.2. Electrochemical Supercapacitors (ESCs)	23
1.2.2.1. <i>Background</i>	24
1.2.2.2. <i>How do Electrochemical Supercapacitor work?</i>	26
1.2.2.3. <i>Electrode Material Technologies and Characteristics</i>	27
1.2.3. Comparison of Electrochemical Supercapacitor and Battery Charging Curves	30
1.3 Objectives of the Present Work	32

CHAPTER 2. *Experimental Techniques*

Abstract	37
2.1. Reagents	38
2.2. Synthetic Techniques	39
2.2.1. Chemical Synthesis of Hybrid Materials	39
2.2.1.1. <i>PAni/MnO₂ Hybrid synthesis</i>	39
2.2.1.2. <i>PPy/MnO₂ Hybrid synthesis</i>	40
2.2.1.3. <i>PAni/V₂O₅ Hybrid Optimization</i>	40

2.2.1.4.	<i>PPy/HCF/V₂O₅ Hybrid Synthesis</i>	41
2.2.1.5.	<i>PAni/HCF/V₂O₅ Hybrid Synthesis</i>	41
2.2.1.6.	<i>PPy/ VOPO₄ Hybrid Synthesis</i>	42
2.2.1.7.	<i>PAni/ VOPO₄ Hybrid Synthesis</i>	42
2.2.2.	Electrochemical Syntheses of Hybrid Materials	42
2.2.3.	V ₂ O ₅ Sol-Gel Synthesis	43
2.2.3.1.	<i>V₂O₅.nH₂O Xerogels</i>	43
2.3.	Chemical Characterization Techniques	43
2.3.1.	Elemental Analysis	44
2.3.2.	Atomic Absorption Analysis (AA)	44
2.3.3.	Analysis by Induced Coupled Plasma (ICP)	44
2.4.	Electrochemical Techniques	45
2.4.1.	Potentiometric Titration	45
2.4.2.	Cyclic Voltametry Technique	45
2.4.3.	Rechargeable Lithium Cells and Electrochemical Supercapacitors	47
2.4.3.1.	<i>Electrodes</i>	49
2.4.3.2.	<i>Data Analysis. Working conditions</i>	50
2.5.	Other Physical-Chemical Characterization Techniques	52
2.5.1.	Scanning Electron Microscopy (SEM)	52
2.5.2.	BET Analyses	52
2.5.3.	TGA Analyses	52
2.5.4.	Fourier Transform Infrared spectroscopy (FTIR Spectroscopy)	53
2.5.5.	X Ray Diffraction (XRD)	53
2.5.6.	Resistivity Measurements	53
2.6.	Taguchi's Experimental Design	54

CHAPTER 3. MnO₂ Hybrids

Abstract	57
3.1. Introduction	58
3.2. PAni/MnO ₂ Hybrid	60
3.2.1. PAni/MnO ₂ Chemical Synthesis	61

3.2.1.1.	<i>Preliminary Experiments</i>	61
3.2.1.2.	<i>Chemical Synthesis</i>	66
3.2.2.	Characterization of Materials from PANi/MnO ₂ reactions	67
3.2.2.1.	<i>Extraction experiments</i>	67
3.2.2.2.	<i>Stoichiometry and Formula Weight of PANi/MnO₂ derivatives</i> ..	68
3.2.2.2.1.	Thermogravimetric Analysis (TGA)	68
3.2.2.2.2.	Elemental Analysis	69
3.2.3.	Study as cathodes in reversible Li cells	70
3.3.	PPy/MnO ₂ Hybrids -----	71
3.3.1.	PPy/MnO ₂ hybrid synthesis	71
3.3.2.	PPy/MnO ₂ characterization	73
3.3.2.1.	<i>FTIR</i>	3
3.3.2.2.	<i>Stoichiometry and formula weight determination</i>	76
3.3.2.2.1.	TGA Analysis	76
3.3.2.2.2.	Atomic Absorption	77
3.3.2.2.3.	Elemental Analysis	78
3.3.3.	Study as Cathode Materials in reversible Li cells	79

CHAPTER 4. V₂O₅ Xerogels

Abstract	-----	83
4.1.	Introduction -----	84
4.2.	Synthesis of V ₂ O ₅ ·nH ₂ O Gel -----	88
4.3.	Determination of V(V) in V ₂ O ₅ ·nH ₂ O Gels -----	88
4.4.	Aging Study of the Gel -----	89
4.5.	Water Content of Gels Used for the synthesis of PANi/V ₂ O ₅ Hybrids -----	90
4.6.	V ₂ O ₅ Xerogels Synthesis-----	92
4.6.1.	X-Ray Diffraction	93
4.6.2.	Infrared Spectroscopy (FTIR)	97
4.6.3.	Rechargeable Lithium Batteries	98
4.6.3.1.	Specific Charge	98
4.6.3.2.	Effect of the presence of Crystalline Phase	99
4.6.3.3.	Cyclability	100

CHAPTER 5. PAni/ V₂O₅ Hybrid Materials

Abstract	105
5.1. Introduction	106
5.2. PAni/ V ₂ O ₅ Hybrid Synthesis	108
5.2.1. Type of Stirring Effect	109
5.2.2. Oxygen treatments	112
5.3. PAni/V ₂ O ₅ Hybrid Characterization	113
5.3.1. XRD (X-Ray Diffraction)	113
5.3.2. FTIR Infrared spectra	115
5.3.3. Scanning Electron Microscope (SEM)	115
5.3.4. BET Analysis	116
5.3.5. Chemical analyses and Stoichiometry determination	117
5.3.5.1. TGA Analysis	117
5.3.5.2. Elemental Analysis	118
5.4. Electrode Fabrication. Comparative analysis of PAni/V ₂ O ₅ Hybrids as composite cathodes in powder, film and vs. Li _x C ₆ anodes	120
5.4.1. Cathode preparation and of Li _x C ₆ anode	121
5.4.1.1. Powder Composite Hybrid Cathodes	121
5.4.1.2. Film Composite Hybrid Cathodes	121
5.4.1.3. Li _x C ₆ anodes	108
5.4.2. Battery Analysis of our Composite Hybrid Cathodes and Composite Anodes	123
5.5. Cyclability Study of the Optimized Hybrids	126

CHAPTER 6. Triple Hybrids

Abstract	133
6.1. Introduction	134
6.2. PPy/HCF/V ₂ O ₅ Triple Hybrid	135
6.2.1. Synthesis	136
6.2.2. Basic Characterization	137
6.2.3. Electrochemical Characterization	139

6.3. PAI/HCF/V ₂ O ₅ Triple Hybrid	140
6.3.1. Synthesis	140
6.3.1.1. Basic Characterization	141
6.3.1.2. Electrochemical Characterization	143
6.3.2. Effect of the order of addition of the inorganic reagents	144
6.3.2.1. Synthesis	144
6.3.2.2. Basic Characterization	145
6.3.2.3. Electrochemical Characterization	146
6.3.3. Effect of the time between the addition of the inorganic reagents	147
6.3.3.1. Synthesis	147
6.3.3.2. Basic Characterization	148
6.3.3.3. Electrochemical Characterization	149

CHAPTER 7. Vanadyl Phosphate Hybrids

Abstract	153
7.1. Introduction	154
7.2. Vanadyl Phosphate Dehydrated (VOPO ₄ ·2H ₂ O)	157
7.2.1. Synthesis	157
7.2.2. Basic Characterization	157
7.3. PPy/VOPO ₄ Hybrids	158
7.3.1. Comparative analysis of synthetic methods.....	159
7.3.1.1. Synthesis	159
7.3.1.2. Basic Characterization	160
7.3.1.3. Electrochemical Characterization	162
7.3.2. Optimization of reaction time	163
7.3.2.1. Synthesis	163
7.3.2.2. Basic Characterization	163
7.3.2.3. Electrochemical Characterization	164
7.3.3. Optimization of the order of addition of the reagents	165
7.3.3.1. Synthesis.....	166
7.3.3.2. Basic Characterization	166
7.3.3.3. Electrochemical Characterization	167
7.3.4. Optimization of the HClO ₄ molar ratio	168

7.3.4.1.	Synthesis	168
7.3.4.2.	Basic Characterization	169
7.3.4.3.	Electrochemical Characterization	170
7.3.5.	Optimization of the pyrrole to vanadyl phosphate ratio.....	171
7.3.5.1.	Synthesis	171
7.3.5.2.	Basic Characterization	172
7.3.5.3.	Physicochemical Characterization	173
7.3.5.3.1.	Scanning Electron Microscope (SEM)	173
7.3.5.3.2.	Resistivity Measurements	174
7.3.5.4.	Stoichiometry Determination	174
7.3.5.5.	Electrochemical Characterization	176
7.3.6.	Final optimization and purification of PPy/VOPO ₄ (PVP11B).....	177
7.4.	PAni/VOPO ₄ Hybrids	179
7.4.1.	Comparative analysis of synthetic methods.....	180
7.4.1.1.	Synthesis	180
7.4.1.2.	Basic Characterization	181
7.4.1.3.	Electrochemical Characterization	182
7.4.2.	Optimization of the order of addition of the reagents	183
7.4.2.1.	Synthesis	183
7.4.2.2.	Basic Characterization	184
7.4.2.3.	Electrochemical Characterization	185
7.4.3.	Optimization of the HClO ₄ molar ratio	186
7.4.3.1.	Synthesis	186
7.4.3.2.	Basic Characterization	186
7.4.3.3.	Electrochemical Characterization	187
7.4.3.4.	Resistivity Measurements	188
7.4.4.	Optimization of aniline to vanadyl phosphate ratio.....	188
7.4.4.1.	Synthesis	189
7.4.4.2.	Basic Characterization	189
7.4.4.3.	Physicochemical Characterization.....	191
7.4.4.3.1.	Resistivity Measurements	191
7.4.4.3.2.	Scanning Electron Microscope (SEM)	191
7.4.4.4.	Stoichiometry Determination	192
7.4.4.5.	Electrochemical Characterization	194
7.4.5.	Electrochemical Studies on sample A15	196

CHAPTER 8. Molecular Hybrids for Electrochemical Capacitors

Abstract	199
8.1. Introduction	200
8.2. Synthesis Background	201
8.3. PAni/SiW12 Hybrids	202
8.3.1. Synthesis of PAni/SiW12 hybrids	202
8.3.2. Characterization of PAni/SiW12	203
8.3.3. PAni/SiW12 Electrochemical Supercapacitors	205
8.4. PAni/PW12 Hybrids	206
8.4.1. Synthesis of PAni/PW12 hybrids	206
8.4.2. Characterization of PAni/PW12	207
8.4.3. PAni/PW12 Electrochemical Supercapacitors	209
8.5. PAni/PMo12 Hybrids	210
8.5.1. Synthesis of PAni/PMo12 hybrids	210
8.5.2. Characterization of PAni/PMo12	211
8.5.3. PAni/PMo12 Electrochemical Supercapacitors	213

CHAPTER 9.- Conclusions

Conclusions	225
-------------	-----

List of Tables

Table I.I.- Schematic structures and chronology of relevant COPs.....	5
Table I.II.- History of the Development of the Electrochemical Capacitor. [62].....	24
Table I.III.- <i>Summary of the characteristics of electrode technological materials</i>	28
Table III.I.- Modified Taguchi experimental design $L_9(3^3)$, for the optimal parameter evaluation in the PANi/MnO ₂ hybrid synthesis.....	63
Table III.II.- Design of the four experiments in order to obtain the PANi/MnO ₂ hybrid, from a reaction between aniline and in situ MnO ₂ (by reaction of permanganate and Mn(II)).....	66
Table III.III.- Summarized data obtain from TGA, of the inorganic part and the organic part + water, of PANi/MnO ₂ samples.....	69
Table III.IV.- Experimental composition from elemental analyses and calculated values for the formula indicated.....	70
Table III.V.- Taguchi's modified experiment design $L_9(3^3)$, to evaluate the optimum synthesis parameters of PPy/MnO ₂ hybrids.....	72
Table III.VI.- Experiments with more amount of initial KMnO ₄	72
Table III.VII.- Data table of FTIR of all PPy/MnO ₂ hybrid samples compared with the bibliographic assign frequencies for polypyrrole.....	74
Table III.VIII.- Comparison between calculated and experimental data of the manganese amount.....	77
Table III.IX.- Summarized data from chemical analysis and calculated formulas for PPy/MnO ₂ hybrids.....	78
Table IV.I.- Samples of all the obtain xerogels with their given treatment.....	93
Table V.I.- X ray powder diffraction data.....	114
Table V.II.- Summarized data from TGA and elemental analysis, in order to determine the stoichiometry and formula weight of the hybrid samples.....	119
Table V.III.- Chemical and Physical characteristics of the different PANi/V ₂ O ₅ hybrids.....	128

Table VI.I.- Molar ratio used in the synthesis of each polypyrrole triple Hybrid samples.....	136
Table VI.II.- Summarized data of the chemical analysis to determine the respective stoichiometry of each polypyrrole triple hybrid samples.....	139
Table VI.III.- Molar ratio used in the synthesis of each polyaniline triple hybrid syntheses.....	141
Table VI.IV.- Summarized data of the chemical analysis to determine the respective stoichiometry of each polyaniline triple hybrid samples.....	143
Table VI.V.- Summarized data of the chemical analysis to determine the respective stoichiometry of each polyaniline triple hybrid samples, optimized based on the order of addition of the inorganic's.....	146
Table VI.VI.- Synthetic optimization conditions for triple polyaniline hybrids, based on the time of addition between the inorganic components.....	148
Table VI.VII.- Summarized data of the chemical analysis to determine the respective stoichiometry of each polyaniline triple hybrid samples, optimized based on the time of addition between HCF and V_2O_5	149
Table VII.I.- Reaction time applied for each simple.....	163
Table VII.II.- Experiments to synthesize PPy/VOPO ₄ hybrids with different HClO ₄ quantites.....	169
Table VII.III.- PPy/VOPO ₄ hybrids synthesized using different molar ratios.....	171
Table VII.IV.- Values of the conductivity calculated from the resistivity measurements made at room temperature.....	174
Table VII.V.- Summarized data of the chemical analysis and tentative formulas of each PPy/VOPO ₄ ·2H ₂ O hybrid samples.....	176
Table VII.VI.- Chemical analysis and formula of the new PPy/VOPO ₄ hybrid	178
Table VII.VII.- Experiments to synthesize PAni/VOPO ₄ hybrids with different HClO ₄ quantities.....	186
Table VII.VIII.- Values of the conductivity calculated from the resistivity measurements made at room temperature.....	188
Table VII.IX.- PAni/VOPO ₄ hybrids synthesized using different molar ratios.....	189
Table VII.X.- Values of the conductivity calculated from the resistivity measurements made at room temperature.....	191

Table VII.XI.- Summarized data of the chemical analysis to determine the respective stoichiometry of each PANi/VOPO ₄ ·2H ₂ O hybrid samples.....	194
Table VIII.I.- Electrochemical conditions of CV for the syntheses of different PANi/SiW12 hybrids.....	203
Table VIII.II.- Electrochemical conditions of CV for the syntheses of different PANi/PW12 hybrid samples.....	206
Table VIII.III.- Electrochemical conditions of CV for the syntheses of different PANi/PMo12 hybrids.....	210
Table VIII.IV.- Summarized data obtained from chemical analyses, and calculated values obtained for the proposed formula weight.....	213
Table VIII.V.- Fabrication procedures for devices assembled with active area electrodes, and active mass electrodes.....	217

List of Figures

- Fig. 1.1.-** Mural painting of the E goddess (represents the relation with the soil and corn) of the ancient Mayan culture, where we can appreciate their famous blue color.
.....3
- Fig. 1.2.-** Schematic representations of the major groups of compounds considered in this work and their combinations to form Organic-Inorganic (OI) and Inorganic-Organic (IO) hybrids.
.....6
- Fig. 1.3.-** Structures of representative examples of polyoxometalates of the heteropolyanion type (a) Keggin structure $[XM_{12}O_{40}]^{n-}$. The $[PMo_{12}O_{40}]^{3-}$ and $[SiW_{12}O_{40}]^{3-}$ anions presents this structure. (b) Wells-Dawson structure $[X_2M_{18}O_{62}]^{n-}$. The $[P_2W_{18}O_{62}]^{6-}$ presents this structure.....8
- Fig. 1.4.-** Schematic diagram, showing the redox insertion mechanisms of conventional COPs, and hybrid materials. a) Shows the typical mechanism for conventional COPs doped with simple small anions, which get inserted upon oxidation (p-doping) and deinserted upon reduction. b) Modified mechanism achieved by anchoring large anions like $[PMo_{12}O_{40}]^{3-}$. Reduction of the hybrid takes place with insertion of cations..... 11
- Fig. 1.5.-** Schematic structure of the IO hybrid based on the intercalation of polyaniline into vanadyl phosphate layers.....13
- Fig. 1.6.-** Schematic Ragone plot for various energy storage and conversion devices. The shaded areas are just indicative and intended for comparison. [45].....15
- Fig. 1.7.-** Specific energy (Wh/Kg) vs energy density (Wh/l) for the different types of normally used batteries..... 17
- Fig. 1.8.-** Schematic drawing of two types of lithium batteries. On top, we show a conventional cell with a metallic lithium anode, and on the bottom a lithium-ion cell using a Li_xC_6 anode. The electron flow indicated corresponds to the discharge processes.....18
- Fig. 1.9.-** Ionic diffusion dimensionality in function with the structure.....21

- Fig. 1.10.-** Schematic of an double layer electrochemical supercapacitor. Where $Q=C\Delta V$, $E=1/2 C (\Delta V)^2$, $C=1/2 [(F/g)wt]$ active material in cell, C= Capacitance of cell, F/g= Farads per gram of active material.....27
- Fig. 1.11.-** Difference of discharge and recharge relationships for a capacitor and a battery: potential as a function of state of charge, Q.....31
- Fig. 2.1.-** Schematic representation of the Potenciostat/Galvanostate used. R is the reference electrode, C the counter electrode, and W the working electrode.].....46
- Fig. 2.2.-** Schematic representation of the three electrode cell setup used for the electrochemical synthesis of polyaniline-polyanions hybrids (electrodes used for the electrochemical capacitors).....47
- Fig. 2.3.-** Swagelok support [8] use for the assembly of rechargeable lithium.48
- Fig. 2.4.-** Schematic representation of battery analyzer. Number from 1 to 4 indicates the four terminals of the apparatus. Number 1 and 2, are the negative electrode terminals; and 3 and 4 corresponding to the positive electrode terminals.....49
- Fig. 2.5.-** Geometry and contact points, used in the Van de Pauw resistivity measurements.54
- Fig. 3.1.-** FTIR spectrum of PAni/MnO₂ derivatives, synthesized with aniline and HMnO₄ (prepared by ionic exchange).....62
- Fig. 3.2.-** FTIR spectrum of sample MnPa9 synthesized with aniline, HClO₄ and KMnO₄, which is very representative of the rest of the hybrid samples. The circles mark vibrational modes assigned to polyaniline oligomers.....63
- Fig. 3.3.-** FTIR spectra of samples PMsa and PMca, synthesized by means of aniline reaction with MnO₂, generated in-situ by reaction of permanganate and Mn(II). The arrows indicate the vibrational modes of polyaniline.....65
- Fig. 3.4.-** FTIR spectrum of the reaction between MnSO₄·H₂O and KMnO₄, with same conditions as for sample PMca.....65
- Fig. 3.5.-** FTIR spectra of samples MP1, MP2, MP3, and MP4 obtain by reaction of aniline with in situ MnO₂66
- Fig. 3.6.-** FTIR spectrum of the solid extracted from PAni/MnO₂ hybrid of sample MP1. The position of the peaks marked correspond to the characteristic oligomer spectrum.....67
- Fig. 3.7.-** FTIR spectrum of sample MP1 washed with ethylic ether. The intensity and position of the marked triplet of vibrational modes belongs to oligomers of 16 units of aniline.....67

- Fig. 3.8.-** TGA analysis of the four PANi/MnO₂ samples: MP1, MP2, MP3 and MP4. The heating rate used for the first three samples was 1°C/min; and for sample MP4, 2°C/min. We have represented in the abscissa axis the time instead of the temperature, in order to appreciate the 500°C isotherm.....68
- Fig. 3.9.-** First discharge of PANi/MnO₂ hybrids, using a discharge density current of I = 4mA/g.....70
- Fig. 3.10.-** Powder XRD of sample MnPy4, which is amorphous representative of all PPy/MnO₂ hybrid samples.....73
- Fig. 3.11.-** FTIR spectra of synthesized PPy/MnO₂ hybrid samples from table III.VI. where the dots represent the vibrational modes of polypyrrole and the arrow Mn-O.....73
- Fig. 3.12.-** FTIR analysis of PPy/MnO₂ hybrids of table III.VII, where the dots represent the vibrational modes of polypyrrole and the arrow Mn-O.....74
- Fig. 3.13.-** FTIR spectra of the experiments where the hybrid PPy/MnO₂ was not formed. Samples: a)MnPy2, b)MnPy3, c)MnPy675
- Fig. 3.14.-** Thermogravimetric analysis (TGA) at 1°C/min in air, of the hybrid PPy/MnO₂ samples. (a)MnPy12, (b)MnPy13, (c)MnPy11, (d)MnPy10, (e)MnPy7, (f)MnPy4,(g)MnPy8, (h)MnPy1, (i)MnPy9, and (j)MnPi5.Py.....76
- Fig. 3.15.-** Correlation between the N% of elemental analysis with the weight loss percentage from TGA analysis (%polypyrrole+%water).for all the samples of PPy/MnO₂ hybrid. The numbers in the graph corresponds to the sample number.....78
- Fig. 3.16.-** In this graph we can see the first cycle charge-recharge for each of the PPy/MnO₂ hybrid samples at C/35. a)MnPy1, b)c)MnPy9 and MnPy5, d) MnPy7, e)MnPy8, f)MnPy4, g)MnPy12, h)MnPy10, i)MnPy13, and j)MnPy11.....79
- Fig. 3.17.-** Graphic representation of the relation between the %Mn with the obtain specific charge of the first charge-discharge cycle. The numbers in the graph corresponds to the sample number.].....80
- Fig. 3.17.-** Schematic representation of composition changes in the PPy/MnO₂ hybrid, during charge-discharge reactions.....81
- Fig. 4.1.-** V₂O₅ structures, (A) crystalline phase indicating the unit cell and the long range bond between V-O, and (B) Sketchy structure of the ab plane of the ribbon like corrugated structure of the vanadium pentoxide (V₂O₅) gel and/or xerogel.....84

Fig. 4.2.- Potential variation during discharge of a cell of crystalline V_2O_5 , like active cathodic material (vs. metallic lithium). We indicate the structural changes suffered by the discharge of V_2O_585

Fig. 4.3.- Proposed mechanism for V_2O_5 gel condensation from vanadate anion [22].....86

Fig. 4.4.- Typical titration curve for the determination of V(V). In the inset we show the derivative graph,.....89

Fig. 4.5.- Aging study of $V_2O_5 \cdot nH_2O$ gel over a period of one year.90

Fig. 4.6.- TGA analysis of $V_2O_5 \cdot nH_2O$ xerogel. We can see in the small deviation graph (a,b,c,d), the successive weight loss stages of hydration water of V_2O_5 xerogel.....91

Fig. 4.7.- Powder X-Ray diffraction of V_2O_5 xerogels under different treatments: A) set treated under oxygen, B) set treated under air, and C) set under argon. The order of each set of diffractograms from top to bottom is the sample treated at $350^\circ C$ to the lowest temperature treatment of $180^\circ C$, excepting the air set which is of $100^\circ C$. The (•) indicates samples treated at $180^\circ C$. The (■) indicates samples treated at $250^\circ C$. The (▲) indicates crystalline samples treated at $350^\circ C$94

Fig. 4.8.- Dependence of temperature and atmosphere treatments of the xerogels vs. the spacings between the layers of V_2O_595

Fig. 4.9.- Water mols present in the different xerogels ($V_2O_5 \cdot nH_2O$), treated at different temperatures and atmospheres.....95

Fig. 4.10.- Infrared spectra of the different V_2O_5 xerogels submitted under different treatments. A) set of xerogels treated under oxygen, B) set under air and, C) set under argon. The vibrational modes marked with (•) belong to V_2O_5 , and with arrows the hydration water.....96

Fig. 4.11.- Infrared spectra of sample treated at $180^\circ C$ under argon(superior) and sample treated at $350^\circ C$ (inferior), where we show the hydration water bands. X is a small peak that belongs to V_2O_5 amorphous phase.....97

Fig. 4.12.- Specific Charge of the 1st discharge of each xerogel, at a cycling velocity of C/6.....98

Fig. 4.13.- Discharge-charge cycle of the V_2O_5 xerogels. Where we can identify the presence of crystalline phase, associated to the development of two differentiated discharge stages. a)xerogels treated in oxygen, b)xerogels treated in air, and c)xerogels treated in argon.....99

Fig. 4.14.- Representation of the cyclability loss (measure as the relative charge loss in 15 cycles) of V_2O_5 xerogels, displayed by atmospheres of treatment. Red range: oxygen, Green range: air, and blue range: argon.....101

- Fig. 5.1.-** Schematic reaction and structure of PANi/V₂O₅ hybrid.....107
- Fig. 5.2.-** Graphic representation of the specific charge when applying a $I = 36.7 \text{ mA/g}$ (C/7.5,2.5Li) rate vs. cycle number for all the different samples of PANi/V₂O₅ hybrids; obtain by different stirring procedures.....112
- Fig. 5.3.-** Comparison of 1st discharge cycle at a rate of C/6, of samples (a) A41TO and (b) A41.....112
- Fig. 5.4.-** XRD diffraction patterns of PANi/V₂O₅ best hybrid samples.114
- Fig. 5.5.-** Infrared spectra of the best Pani/V₂O₅ hybrids. The arrows mark the vibrational modes of polyaniline and the circles the ones assigned to V₂O₅.....115
- Fig. 5.6.-** SEM photographs (3 μm scale): Reference, A33 (turbo-propeller, 3 days), A42 (2 days), A43 (3 days), A41 (1 day), and A41TO (1day, oxygen treatment). A4 series synthesized with mechanical mixer.....116
- Fig. 5.7.-** Graph showing the surface area (BET) of samples A4 vs. time. We also include the reference, A33, P3 and P14 for comparison.....117
- Fig. 5.8.-** TGA analysis of our optimized hybrids, under oxygen. In the inferior left box, we show the first derivative where we can see clearer the weight losses.....118
- Fig. 5.9.-** A42 hybrid infrared spectra, and the soluble colored residue.....122
- Fig. 5.10. -** Comparison of the first charge discharge polarization curves for sample A42 as powder and film, vs. Li_xC₆ or Metallic Li anode. $I = 36.7 \text{ mA/g}$ (C/7.5, for 2.5Li exchange).....124
- Fig. 5.11.-** Comparison of composite cathodes on powder, film, and vs. Li_xC₆ anode. In function of the number of cycles, applying a $I = 36.7 \text{ mA/g}$ (C/7.5,2.5Li) discharge rate.....125
- Fig. 5.12.-** PANi/V₂O₅ cathode comparison of series A4 samples, in successive charge-discharge 100 cycles. C/6 rate.....126
- Fig. 5.13.-** Incremental capacity graph of sample A43, where we can see the degradation through cycling of each part of the PANi/V₂O₅ hybrid.....127
- Fig. 5.14.-** Successive charge-discharge cycles carried out in Li cells at $I = 36 \text{ mA/g}$ (C/6 rate at a voltage range of 3.8-2.1V) of the different PANi/V₂O₅ hybrid simples.....128
- Fig. 5.15.-** Cyclic voltammogram of the washing electrolyte containing the soluble species extracted from the A43 cathodes. (5mV/seg. CE= Pt, W=Pt, and REF=Li.).....129

Fig. 5.16.- Successive charge-discharge cycles carried out in Li cells of the washed cathodes at a C/7.5 rate ($I=30\text{mA/g}$). A43 is the cathode firstly washed, and A43W the second washing130

Fig. 6.1.- Schematic structure of the desired triple hybrid, using polypyrrole as a conducting polymer.....134

Fig. 6.2.- FTIR spectra of each PPy/ V_2O_5 /HCF sample. The red circles indicate the vibrational modes of V_2O_5 , the arrows the ones belonging to polypyrrole, and the rhomb belonging to HCF.137

Fig. 6.3.- Powder XRD of the polypyrrole triple hybrid samples137

Fig. 6.4.- TGA analysis of polypyrrole triple hybrids in argon, heating rate $2^\circ\text{C}/\text{min}$ up to 360°C then isothermal for 6 hours. (derivative shown in inset)138

Fig. 6.5.- Electrochemical characterization in reversible lithium cells of our cathodic polypyrrole hybrid samples, at a slow rate of C/40139

Fig. 6.6.- FTIR spectra for each PANi/ V_2O_5 /HCF triple hybrid sample. The circles indicate the vibrational modes of V_2O_5 , the arrows the ones belonging to polyaniline, and the rhomb belonging to HCF.141

Fig. 6.7.- XRD of the polyaniline triple hybrid samples.....142

Fig. 6.8.- TGA analyses of polyaniline triple hybrids, using the following program: rate $2^\circ\text{C}/\text{min}$ up to 360°C for 6 hours in Argon.143

Fig. 6.9.- Electrochemical characterization in rechargeable lithium cells of our polyaniline triple hybrid samples, at a slow charge-discharge rate of C/40.....143

Fig. 6.10.- FTIR spectra for PANi/ V_2O_5 /HCF samples optimized according to the order of addition of the inorganic components. The circles indicate the vibrational modes of V_2O_5 , the arrows the ones belonging to polyaniline, and the rhomb belonging to HCF.145

Fig. 6.11.- Powder XRD for PANi/ V_2O_5 /HCF samples optimized according to the order of addition of the inorganic components.145

Fig. 6.12.- TGA analyses of polyaniline triple hybrids, optimized according to the order of addition of the inorganic components. The followed program was using a rate $2^\circ\text{C}/\text{min}$ up to 360°C for 6 hours.....146

Fig. 6.13.- Electrochemical characterization in rechargeable lithium cells of our cathodic polyaniline triple hybrid samples, synthesized by changing the order of addition of the inorganic components, at a slow charge-discharge rate of C/40.....147

Fig. 6.14.- FTIR spectra of PANi/ V_2O_5 /HCF samples, optimized according to the time addition between HCF and V_2O_5 . The circles indicate the vibrational modes of V_2O_5 , the arrows the ones belonging to polyaniline, and the rhomb belonging to HCF.....148

- Fig. 6.15.-** Powder XRD for PAni/V₂O₅/HCF) samples optimized according to the time of addition between the inorganic components.....149
- Fig. 6.16.-** Electrochemical characterization in rechargeable lithium cells of our polyaniline triple hybrid samples, optimized based on the time between the addition of HCF and V₂O₅, at a slow charge-discharge rate of C/40.....150
- Fig. 7.1.-** Structure of Vanadyl phosphate dihydrate. The orange tetrahedra is the phosphate group, the green octahedra is the vanadyl group, the red circles are bonded oxygen, and the blue circles are oxygen from water.....155
- Fig. 7.2.-** FTIR spectrum of VOPO₄·2H₂O phase, where each stretching modes is assigned.....157
- Fig. 7.3.-** Powder XRD of VOPO₄·2H₂O sonochemically synthesized. The planes of the structure are indicated in the diffraction pattern. The arrow indicates the peak of the superstructure.158
- Fig. 7.4.-** FTIR spectra of PPy/VOPO₄ hybrid samples, synthesized by different methods. The arrows indicate the stretching modes of PPy present in the hybrid and the circles the ones belonging to VOPO₄ and H₂O.....160
- Fig. 7.5.-** Powder XRD of PPy/VOPO₄ samples synthesized with different methods.....161
- Fig. 7.6.-** First charge-discharge cycle for PPy/ VOPO₄ hybrid samples, synthesized by the chemical method at different temperatures.....162
- Fig. 7.7.-** FTIR spectra of PPy/VOPO₄ hybrid samples, synthesized in different reaction times. The arrows indicate the vibrational modes for PPy, and circles the ones from VOPO₄ and H₂O.....164
- Fig. 7.8.-** Powder XRD of PPy/VOPO₄ hybrids samples, synthesized in different reaction times.....164
- Fig. 7.9.-** First charge-discharge cycle for PPy/ VOPO₄ hybrid samples, synthesized with the chemical method with different reaction times.....165
- Fig. 7.10.-** FTIR spectra of PPy/VOPO₄ hybrids samples, synthesized with different addition order. The arrows indicate the vibrational modes of PPy present in the material and the circles the ones corresponding to VOPO₄ and H₂O.....166
- Fig. 7.11.-** Powder XRD of PPy/VOPO₄ hybrids samples, synthesized by changing the order of addition of the reagents.....167
- Fig. 7.12.-** First charge-discharge cycle for PPy/ VOPO₄ hybrid samples, synthesized by changing the order of addition of the reagents.....168

Fig. 7.13.- FTIR spectra of PPy/VOPO₄ hybrid samples, synthesized with different amounts of acid. The arrows indicate the bands of PPy present in the material and the circles the ones corresponding to VOPO₄ and H₂O.....169

Fig. 7.14.- Powder XRD of PPy/VOPO₄ hybrid samples, optimized according to the acid molar ratio.....170

Fig. 7.15.- First charge-discharge cycle for PPy/VOPO₄ hybrid samples, synthesized by changing the acid molar ratio. We include PVP11B sample for comparison.....170

Fig. 7.16.- FTIR spectra of PPy/VOPO₄ hybrid samples, synthesized with different amounts of nominal pyrrole. The arrows indicate the bands corresponding to PPy and the circles the ones belonging to VOPO₄ and H₂O.....172

Fig. 7.17.- Powder XRD of samples synthesized with different amounts of nominal pyrrole.....172

Fig. 7.18.- SEM photographs of the samples synthesized with different amount of nominal pyrrole. We also include sample PVP11B.....173

Fig. 7.19.- TGA analyses of PPy/VOPO₄ hybrids, synthesized with different amounts of nominal pyrrole. The analyses were carried out in air with a 1°C/min rate, up to 500 for 5 hours.....175

Fig. 7.20.- First charge-discharge cycle for PPy/ VOPO₄ hybrid samples, synthesized with different amounts of nominal pyrrole.....177

Fig. 7.21.- Electrochemical characterization of PPy/VOPO₄ hybrid samples, optimized based on PVP11B. The vertical line marks a change in the constant current used for charge-discharge.....179

Fig. 7.22.- FTIR analyses of PAni/VOPO₄ hybrid samples, synthesized by different methods. The arrows indicate peaks from PAni, and the circles the ones assigned to VOPO₄.....181

Fig. 7.23.- Powder XRD of PAni/VOPO₄ hybrids samples, synthesized with different methods.....182

Fig. 7.24.- First charge-discharge cycle for PAni/ VOPO₄ hybrids samples, made by 2 different methods.....183

Fig. 7.25.- FTIR spectra of PAni/VOPO₄ hybrid samples, synthesized by changing the addition order of the reagents. The arrows indicate the bands of polyaniline and the circles the ones belonging to VOPO₄ and H₂O.....184

Fig. 7.26.- Powder XRD of PAni/VOPO₄ hybrids samples, made by changing the order of addition of the reagents.....185

Fig. 7.27.- First charge-discharge cycle for PAni/VOPO₄ hybrid samples, synthesized by changing the order of addition of the reagents.....185

- Fig. 7.28.-** FTIR spectra for PANi/VOPO₄ hybrids samples, synthesized with different amounts of acid. The arrows indicate the stretching modes of polyaniline and the circles the ones for VOPO₄.....187
- Fig. 7.29.-** Diffraction patterns of PANi/VOPO₄ hybrids samples, with variable amounts of acid used in their synthesis.....187
- Fig. 7.30.-** First charge-discharge cycle for PANi/VOPO₄ hybrid samples, synthesized by changing the acid molar ratio.....188
- Fig. 7.31.-** FTIR spectra of PANi/VOPO₄ hybrid samples, synthesized with different amounts of aniline. The arrows indicate the bands of polyaniline and the circles of VOPO₄.....190
- Fig. 7.32.-** diffraction patterns of samples synthesized with different amounts of nominal aniline.....190
- Fig. 7.33.-** SEM photographs of the samples synthesized with different amount of aniline. We also include sample A15. 5k magnification.....192
- Fig. 7.34.-** TGA analyses of PANi/VOPO₄ hybrids, synthesized with different amounts of aniline. The analyses were carried out with a 1 °C/min rate, upto 500 °C for 5 hours.....193
- Fig. 7.35.-** Electrochemical characterization of samples synthesized with different amounts of aniline, where we can see the specific charge values through successive charge-discharge cycles. For the first 5 cycles the I=10mA/g, and the rest of them with I=20mA/g.....195
- Fig. 7.36.-** Electrochemical experiments over sample A15 in lithium reversible cells, where we can see the specific charge values through successive charge-discharge cycles. First 5 cycles at I=10mA/g, and the rest of them at I=20mA/g for samples A15a (3.8-2.1V) and A15c (3.8-1.5V). For samples A15b (3.8-2.1V) at I=20mA/g.....196
- Fig. 8.1.-** Cyclic Voltammograms (20mV/s) of the heteropolyacids (0.02M aq.) vs. Ag/AgCl. SiW12 [SiW₁₂O₄₀]⁴⁻, PW12 [PW₁₂O₄₀]³⁻, PMo12 [PMo₁₂O₄₀]³⁻.....202
- Fig. 8.2.-** Cyclic Voltammogram carried out to synthesize sample SW2 at a scanning rate of 5mV/s.....203
- Fig. 8.3.-** CV of SW3 and SW4 electrodes, carried out in a 1M HClO₄ solution at 20mV/s.....204
- Fig. 8.4.-** SEM photographs made at x300 for the square photos and x5000 for the circles. a)SW2, b)SW3, and c)SW4.....205
- Fig. 8.5.-** Electrochemical capacitors response over PANi/SiW12 hybrid samples with different current densities. Current density normalized per effective electrode area.....205

- Fig. 8.6.-** Cyclic Voltamogram carried out to synthesize sample PW1E at a scanning rate of 10mV/s.....207
- Fig. 8.7.-** CV of PW1A, PW1C and PW1E electrodes, carried out in a 1M HClO₄ solution at 20 mV/s207
- Fig. 8.8.-** SEM photographs of samples of series PW1 made at x318 for the square photos and x5000 for the round ones. a)PW1A, b)PW1C, c)PW1D, d)PW1E, e)PW1F and f)PW1G.....208
- Fig. 8.9.-** SEM photographs of samples of series PW2 made at x300 for the square photos and x5000 for the round ones. a)PW2A, b)PW2B, c)rigid graphite electrode.....209
- Fig. 8.10.-** Electrochemical capacitors response for PAni/PW12 hybrid samples with different current densities.....209
- Fig. 8.11.-** Cyclic Voltamogram carried out to synthesize PAni/PMo12 hybrid (PMoB) electrode using 2 different scanning rates.....211
- Fig. 8.12.-** CV of PMo12 electrode, carried out in a 1M HClO₄ solution at 20 mV/s.....211
- Fig. 8.13.-** SEM photographs of PAni/PMo12 hybrid electrode samples made at x318 for the square photos and x5000 for the circles. a)PMoA, and b)PMoB.....212
- Fig. 8.14.-** FTIR spectrum of PAni/PMo12 hybrid sample (PMo12), where the arrows indicate the stretching modes of polyaniline and the circles the ones belonging to phosphomolibdic anion.....212
- Fig. 8.15.-** Electrochemical Supercapacitor studies of PAni/PMo12 (sample PMoB). Capacitances are normalized per effective electrode area. Upper graph (a) shows capacitances under different current densities at $\Delta V=1V$. Lower graph (b) shows the successive charge-discharge cycles at $I=1mA/cm^2$, where the first 2000 cycles are carried out with a voltage window of $\Delta V=1V$ and the following 1000 cycles using a voltage window of $\Delta V=1.5V$214
- Fig. 8.16.-** Electrochemical supercapacitor studies of PAni/PMo12 (sample PMoB). Capacitances are normalized per mass of active material. Upper graph (a) shows the capacitance values under different current densities at $\Delta V=1V$. Lower graph (b) shows the successive charge-discharge cycles at $I=125 mA/g$ carried out at a voltage window of $\Delta V=1V$ for new and used electrodes.216
- Fig. 8.17.-** Electrochemical supercapacitor studies of PAni/PMo12 (sample PMoB). Capacitances are normalized per mass of active material. (a) Capacitance vs. current densities with $\Delta V=1.2V$. (b) evolution of capacitance with charge-discharge cycles at $I=400 mA/g$ for the same cell ($\Delta V=1.2V$). (c) First 4 cycles measured at 400mA/g (same cell used for the datum at 400mA/g in graph a, i.e. after 60 cycles under varying current densities).....218
- Fig. 8.18.-** Electrochemical studies over supercapacitors with new electrodes between a voltage range of $\Delta V= 0 \rightarrow 1V$. For the PAni/PMo12 hybrid, the first 2000

cycles we applied a 400 mA/g, the next 300 cycles at 125 mA/g and finally the next 2000 cycles at 400 mA/g. For comparison we show the performance of electrodes based on PMo12 (■), the first 1000 cycles we applied a 400mA/g, the next 300 cycles at 125mA/g.....219

List of Papers

Manuscripts submitted:

“The hybrid PAni/V2O5 system. Studies of synthesis optimization and long-term cycleability in reversible Li and Li-ion cells”. A. K. Cuentas-Gallegos and P. Gómez-Romero. Submitted to J. Electrochem. Soc.

“Molecular hybrids with polyoxometalates and polyaniline applied in Electrochemical Supercapacitors”. A. K. Cuentas-Gallegos, M. Lira-Cantú, and P. Gómez-Romero. Submitted to Adv. Funct. Mat.

Manuscripts in preparation:

“Synthesis and characterization of hybrids based on VOPO₄ and conducting polymers.”. A. K. Cuentas-Gallegos, and P. Gómez-Romero.

“In-situ synthesis of Polypyrrole-MnO₂ Nanocomposite hybrids”. A. K. Cuentas-Gallegos and P. Gómez-Romero.

Articles in press:

“Energy Storage in Hybrid Organic-Inorganic Materials”. P. Gómez-Romero A.K. Cuentas-Gallegos, M. Lira-Cantú, N. Casañ-Pastor. (proceedings of 203rd meeting of the electrochemical society)

“Hybrid Insertion Materials Based on Vanadyl Phosphate or Vanadium Pentoxide, and Conducting Polymers”. A.K. Cuentas-Gallegos, M. Lira-Cantú, R. Vijayaraghavan, N. Casañ-Pastor, and P. Gómez-Romero. (proceedings of 203rd meeting of the electrochemical society)

“Hybrid Materials Based on Vanadyl Phosphate and Conducting Polymers as Cathodes in Rechargeable Lithium Batteries”. A.K. Cuentas-Gallegos, R. Vijayaraghavan, M. Lira-Cantú, N. Casañ-Pastor, P. Gómez-Romero. (Bol. Soc. Es. Ceram. Vidrio.)

Book Chapter *“Electroactive organic-inorganic Hybrid materials. From electrochemistry to multifaceted applications”* K. Cuentas-Gallegos, M. Lira-Cantú, N. Casañ-Pastor, P. Gómez-Romero. P. Cabot editor.

Published papers:

“Hybrid organic-inorganic nanocomposite materials for application in solid state electrochemical supercapacitors”. Pedro Gómez-Romero, Malgorzata Chojak, Karina Cuentas-Gallegos, Juan A. Asensio, Pawel J. Kulesza, Nieves Casañ- Pastor, Monica Lira-Cantú., Electrochem. Commun., 5, 149-153, 2003.

“Influence of Thermal Treatment and Atmospheres on the Electrochemistry of V_2O_5 as Lithium Insertion Cathode”. A. K. Cuentas-Gallegos and P. Gómez-Romero. New Trends in Intercalation Compounds for Energy Storage, Ed. C. Julien, J.P. Pereira-Ramos and A. Momchilov, NATO Science Series, Vol.61, 535-538.

“Study of Hybrid Cathode Materials and Vitreous Anodes.Characterization in Lithium Ion Cells”. A.K. Cuentas-Gallegos, M. Rosa Palacín,MT Colomer J.R. Jurado, P. Gómez-Romero. Bol. Soc. Es. Ceram. Vidrio., 41(1), 115-121, 2002.

“Hybrid Electrodes based on Polyaniline/ V_2O_5 for the development of plastic lithium batteries” Lira-Cantu, M.; Cuentas-Gallegos, A.K.; Torres-Gómez, G.; Gómez-Romero, G. Bol. Soc. Es. Ceram. Vidrio, 39(3), 386-390, 2000.

Chapter 1

Introduction

Abstract:

The study of hybrid materials based on organic conducting polymers and electroactive inorganic species merges two areas of chemistry (organic and inorganic), trying to bring together the best properties of each component in order to enhance their functionality. They can be classified in three major groups: OI (organic-inorganic), IO (inorganic-organic), and nanocomposite hybrids. These electroactive hybrids represent novel concept materials with properties and possible applications that need to be explored. In the present work we center on different energy storage applications that could benefit from the development of novel materials, namely, lithium rechargeable batteries and electrochemical supercapacitors.

1.1 HYBRID MATERIALS

Organic-inorganic hybrid materials represent the natural interface between two worlds of chemistry (organic and inorganic) each with very significant contributions to the field of materials science, and each with characteristic properties that result in diverse advantages and limitations. The main idea when developing hybrid materials is to take advantage of the best properties of each component that forms the hybrid, trying to decrease or eliminate their drawbacks getting in an ideal way a synergic effect; which results in the development of new materials with new properties.

The art of combining dissimilar components to yield improved materials is not new; in fact it goes way back to ancient construction materials like Adobe [1]. Adobe was used to build houses and buildings and was made from a mixture of clay (inorganic) and straw (organic), where the straw provides the mechanical properties for clay. Nevertheless, the modern concept of hybrid materials goes way beyond the concept of a mixture between their components, actually falls between the concept of a mixture and a compound. A compound is formed by carrying out a chemical reaction between their components, where the properties of each part are eliminated to form a new material with different properties. In a mixture, as we already mention, a physical interaction between their components is involved. The hybrid concept falls into a category where the interphase between their components is increased compared to a mixture, and the interaction is at a molecular level.

Other example of an ancient hybrid material is the blue Maya color that still maintains its bright color since 1300 years ago (see figure 1.1). Aside the beauty of this blue color paint and that is harmless to the environment, it is extraordinary resistant to dilute acids, alkaline solvents, oxidants, reductors, moderate temperatures, and even bio-corrosion. The ancient Mayas worship the color blue and modern scientists [2] have recently discovered why this color has kept its brightness through centuries, with the help of new scientific techniques like HRTEM, EELS, and XRD. The results have shown that the blue Maya contains clay, mainly paligorskite mixed with some sepiolite and monmorillonite that by their own are white. Also, contains indigo (vegetal pigment) present in plants of gender *indigofera* (xiuquilit plant) and *Isatis*, which were known by antique civilization of Asia, Egypt, Europe and Pre-columbian America. But indigo is not to resistant to chemical and physical agents. The key for obtaining this color (re-discovered by scientists) was the heat treatment at 150

°C during 20 hours. Now it is known that this technique produces a special crystallization, where the paligorkite crystals form a characteristic matrix where two types of nanometric particles are anchored, which are the ones responsible for its resistance and color permanence. One type of particles is located in the interior of the matrix, which are metallic residues, mainly iron oxide, while the particles located in the surface contain silicon oxide. From all this we know that the Maya's were a very refined connoisseurs of Chemistry. This antique technique has modern applications and a lot of companies have shown interest

in the Maya's technology recently discovered, with the objective of producing paintings of all colors. This Mayan blue resembles more the modern concept of Hybrid materials.

This modern concept of "organic-inorganic hybrid materials" emerged only very recently, when the research turned to more sophisticated materials with a higher added value, associated to the development of composites and molecular materials where the organic and inorganic component interact at a molecular level as we already mention. [3]

The first interest in the development of hybrid materials was mainly based on the design of hybrid polymers with special emphasis on structural hybrid materials. A variety of silicates, polysiloxanes etc. modified with organic groups or networks for the improvement of mechanical properties, were the first type of hybrid materials investigated.

The expectations for hybrid materials go further than mechanical strength, thermal and chemical stability. So, in addition to those structural materials and applications, many recent efforts have centered on the design of other types of hybrid materials which explore other fields as: Magnetic hybrids (tricarboxilic substituted radical and Cu ions [4]), Electronic hybrids used in electronics (transistors, diodes), and *Functional* Hybrids which are the ones that we will focus on this thesis.



Figure 1.1.- Mural painting of the E goddess of the ancient Mayan culture (represents the relation with the soil and corn), where we can appreciate their famous blue color.

Chemical activity is the main characteristic of functional hybrid materials. They bind the chemical activity of their components by exploring their optical and electrical properties, luminescence, ionic conductivity, and selectivity, as well as chemical or biochemical activity, giving way to materials that can be applied for: sensors, selective membranes, all sorts of electrochemical devices, from actuators to batteries or electrochemical supercapacitors, supported catalysts or photoelectrochemical energy conversion cells, etc. In these functional materials mechanical properties are secondary (still also important) and the emphasis is on reactivity, reaction rates, reversibility or specificity. The hybrid approach can also be useful in this context by combining organic and inorganic species with complementary properties and reactivities. [1]

Research in the topic of hybrid materials involves challenges and opportunities. The most important challenge is managing to synthesize hybrid combinations that keep or enhance the best properties of each of the components while eliminating or reducing their particular limitations, having the opportunity to develop new materials with synergic behavior. This behavior leads to the improvement in performance or to the encounter of new useful properties. There is no doubt that hybrid materials frequently involves a combination of components that have been carefully studied in their respective fields and provide an additional dimension to their properties in becoming part of the hybrid compound.

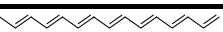
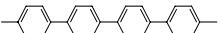

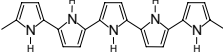
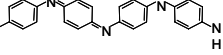
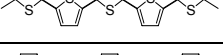

In the hybrid approach there is an immense variety of adducts that can be formed between organic and inorganic species. Taking into account the great diversity of extended and molecular inorganic species, small organic molecules and available polymers for the design of these hybrid materials, it is clear that the variety of combinations is tremendously enormous. The wide range of possible hybrids would include innovative combinations, starting from inorganic clusters, fullerenes or metal nanoparticles dispersed in organic polymers to organic and organometallic molecules, biomolecules or enzymes dispersed in inorganic sol-gel polymers, or macrocycles or polyethylene oxide chains intercalated into silicate minerals. The first group of hybrids studied in a systematically way from a basic point of view, were the ones that consisted on the intercalation of small organic molecules into layered or channeled inorganic solids. Even though these studies were important, the resulting adducts in essence were not functionally designed nor use as materials. However, nowadays the

research carried out in these organic-inorganic systems has increased, keeping in mind their possible application as functional materials.

The work developed in our group and this thesis in particular, is centered on a particularly fruitful and wide group of hybrid functional materials based on conducting organic polymers (COPs) as components. This category alone accounts for a large number of materials and applications; their functionality is based on the electroactivity property of their components, in order to be used as electrodes for energy storage devices.

From the last two decades up to the Nobel Prize in 2000 awarded to A.J. Heeger, A.G. McDiarmid and H. Shirakawa, conducting organic polymers have suffered a dramatic transition from chemical curiosities to revolutionary new materials. And as such, they have deserved great attention and study on their own. Indeed, the field has boomed in such a way that recent reviews tend to center on particular polymers or applications. Table I.I shows some of the polymers which will be discussed in this work. The immense majority of reports dealing with COPs materials involve the study of p-doped polymers, most frequently polypyrrole (PPy), polyaniline (PAni) or polythiophene (PT) and their derivatives. Among their properties and applications the most frequently studied are those related to their semiconductivity and electroactivity and range from their use as plastic conductors or Light-Emitting Diodes (LEDs), to their use in energy storage applications. Important as they are on their own, the combination of COPs with a wide variety of available inorganic species with chemical, photochemical or electrochemical activity can lead to numerous of hybrid functional materials some of which will be described in this thesis.

Table I.I. Schematic structures and chronology of relevant COPs

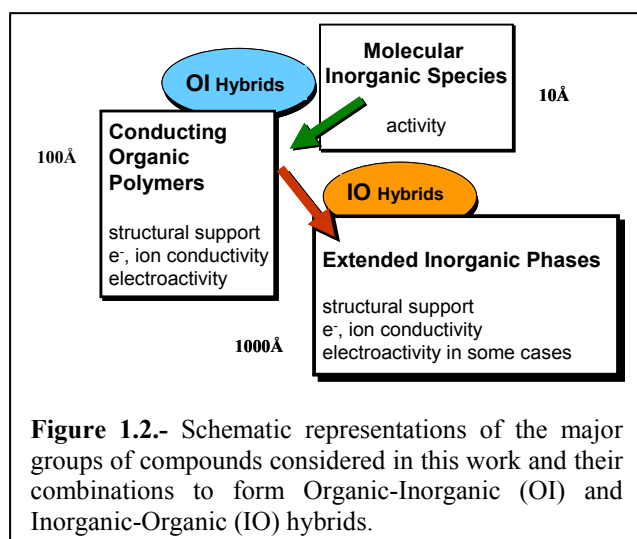
Name	Label	Year^a	Structure^b
<i>Polyacetylene</i>	PAC	1977	
<i>Poly(p-phenylene)</i>	PPP	1979	
<i>Poly(p-phenylenevinylene)</i>	PPV	1979	
<i>Polypyrrole</i>	PPy	1979	
<i>Polyaniline</i>	PAni	1980	
<i>Polythiophene</i>	PT	1981	
<i>Polyfurane</i>	PF	1981	

1.1.1 Classification

Hybrid materials can be classified by using several criteria's based on their field of application (as we mention above) or on their chemical nature. However, if we base this classification on their chemical nature it would result more useful to distinguish common characteristics that would help us understand related behaviors and properties.

A first classification was proposed by P. judenstein et. al.[3] based on the bonding chemical nature between the organic-inorganic interphase. This classification consists of two major groups: Class I where organic and inorganic components are embedded and only weak bounds (ionic bonds, hydrogen bonds or Van der Waals interactions) give the cohesion to the whole structure; and in Class II the two components are linked together through strong chemical bonds (covalent, ionic-covalent or coordination bonds). Even though this is a very simplified classification it is helpful as a first approximation to sort the complexity of a wide variety of systems.

On the other hand, for the analysis and discussion of the *Electroactive* hybrid materials (Functional) considered in this thesis work we will classify them into three groups (two major groups and a category between them) depending on the type of matrix and guest phases. [1] The first group named "OI" (organic-inorganic) hybrid materials consists of an organic matrix (conducting organic polymeric matrix) where the inorganic specie is the guest molecule; the second group named "IO" (inorganic-organic, intercalation compounds) hybrid materials where the matrix is the inorganic electroactive species, and the organic part of the hybrid is the guest molecules (Figure 1.2); and finally falling at the frontier between these two major groups we can find a



type of hybrid material where non of the organic or inorganic components constitutes the matrix nor the guest molecules, which will refer to "nanocomposite" materials. These nanocomposite hybrids are a remainder of Nature's resistance to conform to our otherwise convenient classification schemes.

In addition to the mentioned classification, figure 1.2 shows that depending on the nature of the inorganic species, which will form our hybrid materials, can be either molecular or extended. This will obviously have an influence on the nature of the hybrid compounds, a field in which the 10 Å molecular dimensions, the 100 Å polymer chain dimension and the 1000 Å crystal grain dimension will need to be considered altogether.

In these three categories we can find examples of hybrids with useful combination of properties and applications, which will be discussed for clarity in the following sections.

1.1.1.1 Organic-Inorganic (OI) materials

In this section we will describe and discuss hybrid functional materials where the inorganic molecules will generally contribute with their chemical activity and will need the structural support of COPs (matrix) to become part of a useful solid hybrid material with the added functionality.

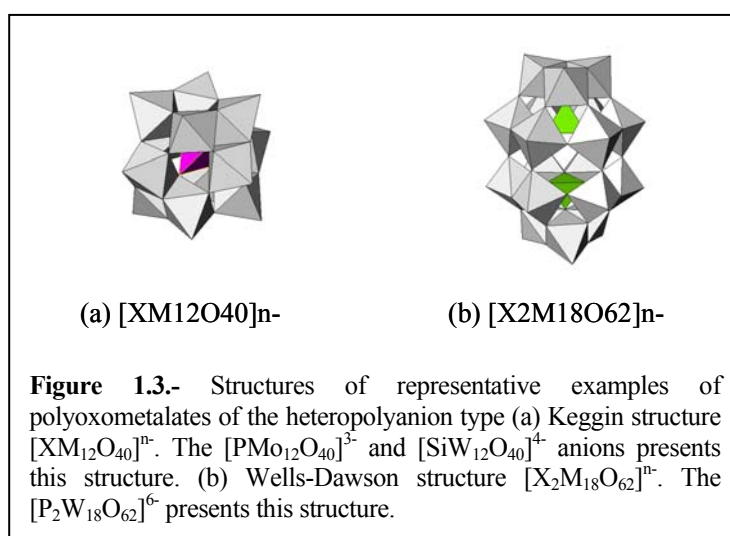
The introduction of molecular inorganic species into a COP network can be accomplished by using two different general approaches: the covalent link approach, and taking advantage of the doping process of COPs. [1]

The covalent link approach relies upon the introduction of suitable coordination sites, groups or molecules which could lead to the formation of metal complexes. These ligands or molecules can get integrated to the polymer chain as functional groups, by means of covalent bonds or by copolymerization with the usual monomers. Using the classification according to Judeinstein et. al. [3] this approach leads to Class II hybrids, where the inorganic centers are firmly linked to the polymer network. Deronzier and Moutet have recently reviewed this class of hybrids for polypyrrole films.[5] This approach has been extensively studied for polypyrrole and polythiophene. In the case of polyaniline, this method encounters more limitations due to the high reactivity of the amino group.

The approach used by taking advantage of the doping process of COPs involves the introduction of holes (p-doped) or electrons (n-doped) into their conjugated network with an accompanied incorporation of charge-balancing species into the structure (anions for p-doped and cations for n-doped). The incorporation of active ionic species as dopants is possible either by ionic exchange or by in-situ incorporation of the active species during polymerization. Given that p-doped COPs

have been more extensively studied, the literature abounds in active-anion doping used in place of, or in addition to, simple inert anions (ClO_4^- , BF_4^- , SO_4^{2-} etc...). The same approach is viable for the introduction of active cations into n-doped polymers. This doping approach results in the formation of less strongly bounds (i.e. class I hybrids) having the advantage of a greater simplicity and versatility, and has permitted the systematical preparation and study of hybrids containing a broad diversity of anionic transition metal complexes such as: tetrachloroferrate, hexacyanoferrate (HCF), and other cyano-metalate complexes, coordination compounds such as oxalatometalates or EDTA complexes, tetrathiomolybdate and macrocyclic compounds like metal phthalocyanine or porphyrine complexes. Within polynuclear metal complexes, polyoxometalates have been by far the most commonly studied. These oxide clusters have been incorporated or anchored into polyacetylene [6], polypyrrole [7,8], poly(N-methylpyrrole) [9], polyaniline [10,11], and polythiophenes [7,12].

Polyoxometalates are small oxide clusters that have been traditionally considered within the framework of molecular chemistry because of their size and solubility. They are complex molecules where their structure consists of several metallic ions coordinated by shared oxide ions forming a highly symmetrical metal oxide. In Figure 1.3 we show two of the most common and extensively studied structures found for these type of clusters, the so-called Keggin structure conforming to the formula $[\text{XM}_{12}\text{O}_{40}]^{n-}$ and the Wells-Dawson structure $[\text{X}_2\text{M}_{18}\text{O}_{62}]^{n-}$.



Polyoxometalates can be classified as Isopolyanions or Heteropolyanions depending on the number of different types of atoms aside from oxygen. In general, Isopolyanions can be described by the general formula $[M_mO_o]^{-p}$, whereas Heteropolyanions are characterized by the formula $[X_xM_mO_o]^{-q}$, M is molybdenum or tungsten, less commonly Vanadium, Niobium, or Tantalum; and X in heteropolyanions could be Si^V , P^{IV} , B^{III} , or V^V . [13] Heteropolyanions constitute a special class of polyoxometalates where XO_4 tetrahedral is the center of the molecule surrounded by MO_6 (M_3O_{13} connected by sharing edges and to the XO_4 center by sharing corners) octahedrons. The number of octahedrons in heteropolyanions is well defined and varies typically from 12 to 48 with a corresponding increase in their size from a diameter of 10 Å for the Keggin structure (Figure 1.3a) to ca. 25Å for the Wells-Dawson's structure (figure 1.3b), although larger clusters are known.

Polyoxometalates present therefore a state of aggregation that makes of them a natural link between the chemistry of extended oxides and the chemistry of monomeric molecules. In addition, their redox, electrochemical and photochemical properties are also parallel to those of related oxides. [1] Heteropolyanions present very interesting molecular properties that are comparable from those of related extended oxides, as their electrochemical activity, electrochromism, photoactivity, magnetic and catalytic properties. Their application is restricted to their molecular nature and solubility. By exploring the hybrid material concept polyoxometalates can be integrated in a material that allows the harnessing of these molecular properties, putting them to work in applications previously unfeasible to these clusters.

The outcome of anchoring heteropolyanions into conducting organic polymers is a hybrid material with the processability and polymeric nature of the matrix and the added activity of the cluster. The permanence of the clusters in these *OI* hybrid materials during possible redox reactions is essential in order to be useful for an application. There are two major points that have to be considered when forming a hybrid based on COPs and electroactive doping agents: 1) spatial distribution of the inorganic doping molecules and their concentration within the polymer matrix, which can vary widely depending on their synthesis conditions; and 2) related to the reversibility nature of the doping process.

The amount of active anions that can be anchored to COPs in the hybrid material is limited by their doping level; but the presence of other (inactive) anions in the synthesis or doping medium can decrease the amount of active species in the hybrid. On the other hand, we must take into consideration that different applications

will require different necessities on the design of a particular material, its form and composition. Earlier work carried out on polyoxometalate-doped COPs was designed for the preparation of supported catalyst, where the interest was to have POMs on the surface of the material. In these cases the concentration of polyoxometalates was secondary, counteranions like ClO_4^- from the acidic medium or HSO_4^- resulting from the reaction of aniline with persulfate would compete with polyoxometalate anions in the doping process of the polymers, reducing drastically the effective amount in the final hybrids. In this direction, Hasik et al. [14,15] studied two possible ways to introduce heteropolyanions into PANi: (i) by direct incorporation “in-situ” of POMs during the polymerization of aniline, and (ii) by acid-base doping of the previously polymerized PANi base. They showed that the two-step method (ii) gave way to more active catalytic material thanks to the concentration of heteropolyanions at the surface due to their delay diffusion. This example highlights the importance of the application-oriented choices regarding to the synthetic methods.

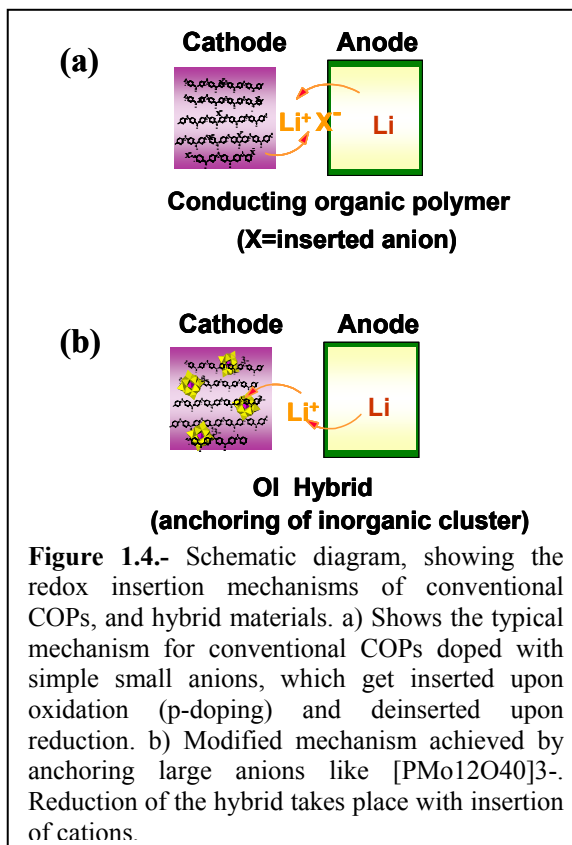
Alternatively, when the application requires bulk materials where the amount of active species is crucial, an optimal doping of the polymer must be essential to increase the amount of incorporated anions, their distribution and the conductivity of the hybrid. In order to introduce more amounts of heteropolyanions, we must consider avoiding the presence of inactive anions, due to a possible competition for the doping process of the polymer. These bulk *OI* hybrid materials are applied for instance for energy storage, where up to one molecule of Phosphomolybdate anion ($[\text{PMo}_{12}\text{O}_{40}]^{3-}$) per nine aniline rings can be anchored into the corresponding hybrid [16,17] (comparing with the maximum value expected of 1 $[\text{PMo}_{12}\text{O}_{40}]^{3-}$ per 6 aniline rings). For the case of PPy the maximum expected value is of one $[\text{PMo}_{12}\text{O}_{40}]^{3-}$ per nine pyrrole rings was experimentally attained, [16,18] while for the case of hexacyanoferrate hybrids up to one $[\text{Fe}(\text{CN})_6]^{3-}$ anion per 10 pyrrole rings was obtained [18] (the optimal expected value is of 1 molecule per 9 pyrrole rings).

These *OI* class I hybrids (loosely bound) could experience the deinsertion of the inorganic active species upon reduction from the conjugated polymer, which affects the reversible nature of the doping process. This would only correspond to the inverse process that takes place during oxidative doping with insertion of anions. For instance, in a rechargeable Li cell or electrochemical supercapacitor that requires redox cycles, this deinsertion effect could take place (figure 1.4a).

The size of the doping anion is determinant to avoid the deinsertion process. For instance, p-doped COPs containing simple conventional anions (relatively small) such as $[\text{ClO}_4^-]$ do suffer the deinsertion of those anions upon reduction. In contrast, large anions with high negative charge will presumably have lower diffusion coefficients within the polymeric matrix and will be more likely to stay. Indeed, polyoxometalates are perfect examples of a large anion; they get effectively anchored within PANi, PPy, PT or even PAc matrices. The verification for this anchoring process is varied and has included cyclic voltammetry of the hybrids as well as quartz-crystal microbalance studies.

The retention of large active anions in these hybrid materials upon reduction in Li cells, forces the insertion of cations for the needed charge balance, with the inverse process of cation expulsion taking place upon reoxidation, converting p-doped polymers into cation-inserting redox materials (figure 1.4b). This cation based mechanism was discovered by analyzing Li after a discharge of a PANi/PMo12 hybrid electrode showing the incorporation of lithium ions corresponding well to the amount of charge involved in the redox reaction [17]. If the retention of the anions is not accomplished, they would form a salt with lithium (figure 1.4a) resulting in a non rechargeable lithium cell.

The possibility of converting p-doped COPs into cation-inserting polymers opens new possibilities for their application, for example as selective membranes or sensors, or for their integration in energy storage devices such as electrochemical supercapacitors or rechargeable lithium batteries most commonly based on cation-producing anodes and a source-sink mechanism, which prevented the efficient use of conventional COPs due to their anion-insertion mechanism. [1]



1.1.1.2 Nanoparticles dispersed in Conducting Organic Polymers. Hybrid nanocomposites.

As we mention in section 1.1.1., some hybrid materials fall at the frontier between *OI* and *IO* hybrids, defying any classification. In this *Nanocomposite* hybrids none of the phases (organic or inorganic) dominates the structure. For instance, colloidal nanometric particles of metals or metallic compounds disperse in COPs constitute a perfect example of these *Nanocomposite* materials [20]. In these materials, the inorganic nanoparticles do not act as the matrix for the intercalation of organic polymers neither as guest species due to their size. Therefore, these hybrid materials could be considered as real composite materials where each part of the hybrid maintains its own structure with increased interfacial interaction due to the nanometric particle size.

Within this category we can identify two major groups: a) conformed by nanosized metal particles dispersed in COPs, and b) where the nanodispersed phase is an oxide. In the first category the metals that are commonly used are precious metals from group 10 like Pd and Pt [21], resulting in hybrid materials designed for catalytic purposes (proton and oxygen reduction, hydrogen oxidation, and hydrogenation reactions). Aside metals, there are also other interesting studies on dispersions of other active elements such as C and S for energy storage applications, for electrocatalysts used for environmental remediation in Cr(VI) reduction, or for sensors and “artificial-noses” [1]. In the second category of *composite* hybrid materials it has been reported the use of colloidal particles of transition metal oxides (γ -Fe₂O₃ [22], MnO₂ [23], CuO [24], TiO₂ [25,26] and WO₃ [27]), tin oxide [28] and silica [28]. In addition, recent reports have extended this family of hybrid composites to other colloidal semiconducting particles such as CdS, CdSe and copper or silver halides for solar energy applications.[1]

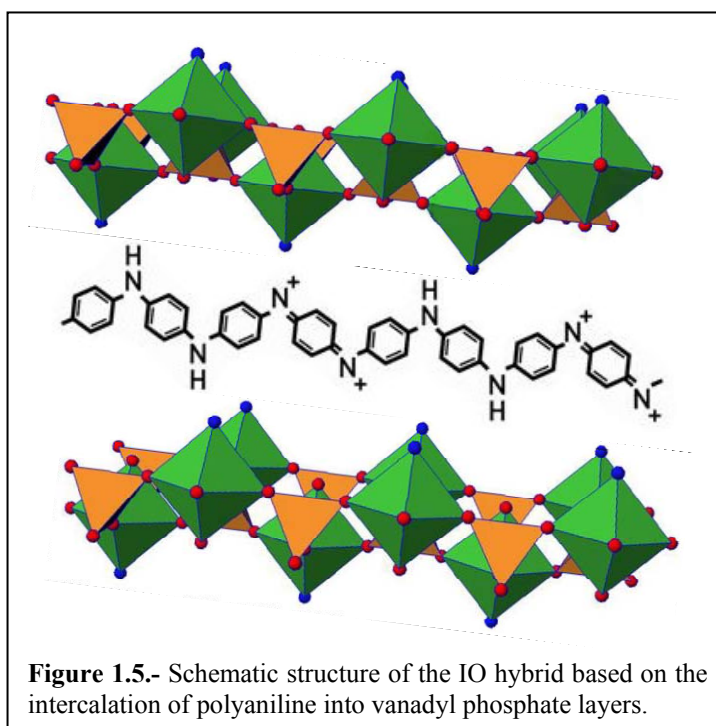
1.1.1.3 Inorganic-Organic (IO) materials

The last classification group referred as *IO* hybrids, the inorganic phase fulfills in principle the structural task (matrix) for the organic component (COPs). Regardless of the relatively large molecular weights of COPs, they can play in certain cases the role of intercalated guest molecules inserted into Van der Waals gaps, adapting to the structure of layered or channel inorganic phases. In some cases the inorganic structure in the hybrid is poorly crystalline resulting in a long range structure difficult to detect. Also, we should consider that this inserted polymer into the inorganic matrix is not a true host-

guest system, due to a difficult deinsertion (reversible) process of the polymer from the inorganic phase. In fact, the key to synthesize these *OI* hybrid materials rely upon the irreversible in-situ polymerization of the resultant monomers once they intercalate into the inorganic host or otherwise on the simultaneous formation of both organic and inorganic polymeric structures. If COPs are previously formed, long chains and high molecular weights are obtained, preventing their effective diffusion into the host structure.

Some examples of these types of *IO* hybrid materials include insertion compounds of COPs in layered oxides such as V_2O_5 , or MoO_3 , layered transition metal sulfides like MoS_2 , chlorides like $RuCl_3$, and oxychlorides like $FeOCl$, silicates and phosphates (α - $VOPO_4$ [30-32] VO_2PO_4 , $CdPS_3$ and $NiPS_3$) as well as the insertion within the channels of zeolitic solids.

The formation of *IO* intercalation materials based on COPs inserted into layered inorganic host takes place with the initial intercalation of the corresponding monomer into the inorganic layered structure, followed by its polymerization. The monomers polymerize due to the strong oxidizing nature of the inorganic matrix. We must mention that the polymer inserted is p-doped (partially oxidized) and the host suffers a partial reduction resulting in a n-doped (partially reduced) electrical conducting host. This mutual doping process takes place during redox intercalative polymerization, giving way in principle, to a material with a double conduction mechanism. In figure 1.5 we show a schematic structure of one of these *IO* hybrids, specifically the one formed between vanadyl phosphate and polyaniline, which has been characterized in this work (Chapter 7) as a Li insertion cathode for the first time.



One of the most extensively studied and better characterized *IO* systems is the family of hybrids based on V_2O_5 as the inorganic host. In fact, a few major lines of work dealing with several hybrids: PANi- V_2O_5 [33-37], PPy- V_2O_5 [38-40] and PT- V_2O_5 [41,42]. For a given hybrid, the inorganic starting matrix could be either crystalline V_2O_5 or the quasi-amorphous V_2O_5 xerogel. Most studies have been based on the production of hybrids interacting at the molecular level with reduced kinetic barriers for their formation.

1.2 ENERGY STORAGE DEVICES AND APPLICATIONS

Energy generation, which to date has largely been based on fossil fuels, is a major source of anthropogenic greenhouse gas emissions and other pollutants. Clearly, the world is set to make major changes to its energy supply and utilization systems. Nevertheless, future energy generation must be sustainable in terms of cost, fuel, resource availability and environmental acceptability. In addition, energy must be generated and supplied in the form and quality to meet the end-user requirements. Much effort is being spent on sustainable energy supply through actions such as the development of more efficient energy generation technologies. Moreover, no single technology in isolation is likely to fulfill the future energy and environment needs of our society. Novel energy conversion devices such as fuel cells and renewable energy devices such as present photovoltaic or future dye-sensitized solar cells will need the support of efficient energy-storage technologies. Rechargeable lithium batteries and electrochemical supercapacitors are two of the most prominent technologies in this respect.[43,44]

Not only in local power generation but also in transport applications, novel energy generation technologies are set to play key roles in the near future. The use of advanced electrochemical supercapacitors/battery systems in hybrid electric vehicles, and fuel cells to power passenger cars, buses, light commercial trucks and heavy transport will be some examples. Most major car manufacturers (Ford, General Motors, Daimler Chrysler, Toyota, Honda, Nissan, Renault, etc.) are now showing interest in the development of an all-electric-and/or hybrid-drive trains utilizing fuel cell technology, either in isolation or in combination with electrochemical supercapacitors and/or batteries.[43] It is important to underscore the complementary nature of the

different energy storage devices and the need to develop them in parallel. Figure 1.6 shows the typical energy storage and conversion devices in the so called Ragone Plot, in terms of their specific energy and power [45].

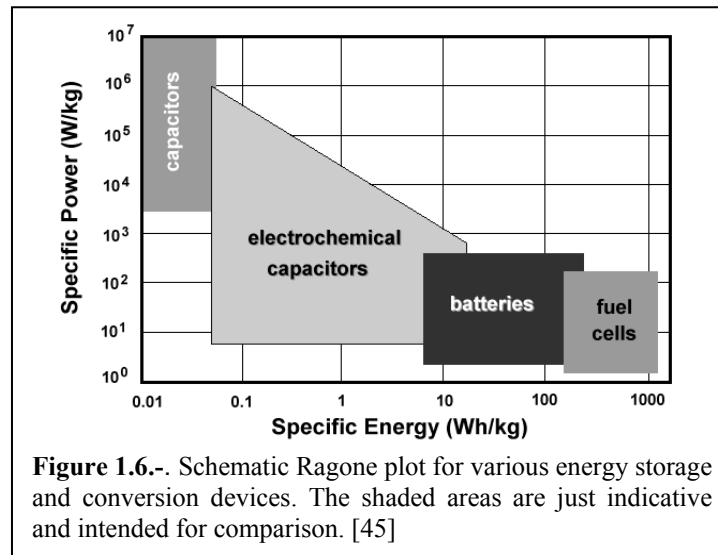


Figure 1.6.-. Schematic Ragone plot for various energy storage and conversion devices. The shaded areas are just indicative and intended for comparison. [45]

Batteries and low temperature fuel cells are typical low power devices whereas conventional capacitors may have a power density of $>10^6$ watts per dm^3 but very low energy density. Thus, electrochemical supercapacitors (ESCs) may improve battery performance in terms of power density or may improve capacitor performance in terms of energy density when combined with the respective device. In addition, electrochemical supercapacitors are expected to have a much longer cycle life than batteries because no chemical charge transfer reactions (or a negligibly small) are involved. [45]

Finally, we would like to mention another important trend within the field of energy storage and conversion, namely, the development of alternative designs for electrodes and batteries, exemplified by the very important efforts taking place internationally to develop plastic batteries, ultrathin systems or microbatteries, all of them fields in which the type of hybrid materials presented in this thesis could be very viable.

1.2.1 Lithium Rechargeable Batteries

Batteries are the most likely medium for the storage of renewable electricity and, indeed, are already used in conjunction with wind turbines and photovoltaic installations. On the other hand, small lithium batteries are now widely employed in portable electronic devices. A few large lithium-ion battery modules have been made as prototypes for electric-vehicle power sources, but as yet these have technical problems and are costly.[44]

1.2.1.1 Background

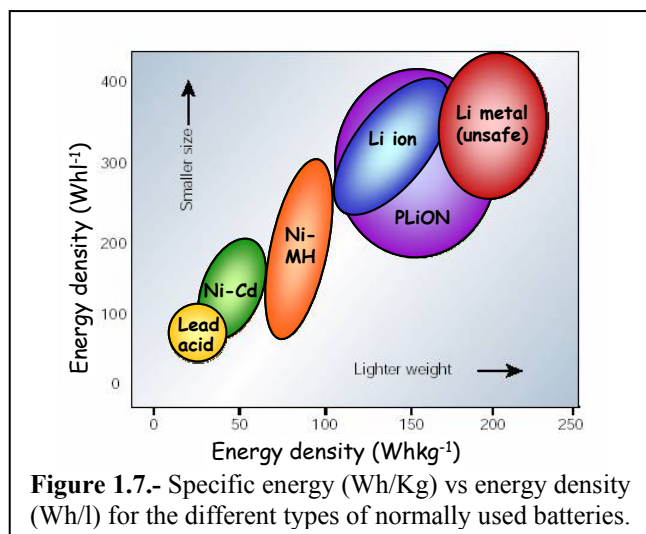
Lithium rechargeable batteries belong to the secondary battery type, which are based on electrochemically reversible systems. When they are discharge they give energy (galvanic cells) and during the recharge they behave like electrolytic cells.

The development of batteries based on lithium anode dates back to the 1950's, when it was discovered that lithium was stable under different non-aqueous electrolytes (propylene carbonate, molten salts, etc.). This stability was attributed to a passivation layer, which prevents the direct chemical reaction between metallic lithium and the electrolyte; but permitting the diffusion of lithium through the ionic conductor electrolyte during the discharge. The commercialization of primary lithium batteries started on the 1960's and 1970's for military applications, and because of its high specific charge and variable discharge rate they quickly found applications also as power sources for watches, calculators or for implantable medical devices [46]. The recharge process of the first used lithium anodes, presented difficulties derived from lithium dendrites formation on the anode, resulting on problems of safety and possible internal short-circuits [47]. In the same period of time, variable inorganic compounds were shown to react with alkali metals in a reversible way. The discovery of such materials, which were later identified as intercalation compounds, was crucial in the development of high energy rechargeable Li systems. In 1973 the first rechargeable lithium battery was developed. It was based on a NiOOH cathode and it was followed by other systems with different cathodic materials in combination with lithium anodes. The key factor on these systems is the active material used as cathode. In principle, it was considered that these phases should have an open structure capable of reversibly accepting ions without significant structural changes. So, a great variety of layered phases where used as cathodes in lithium reversible cells. Some examples were: transition metal dicalcogenides like TiS_2 [47], and some oxides like V_6O_{13} and

V_2O_5 . In 1972 Exxon embarked on a large project using TiS_2 as the positive electrode, Li metal as the negative electrode and lithium perchlorate in dioxolane as the electrolyte. [46] On the other hand, in 1987 Allied-Signal Inc. announced work on the first lithium battery using polyaniline as cathode followed by Bridgestone Co. in 1989.

Japan soon had five

companies that worked with polyaniline in the field of batteries [48]. However, as we mention before, p-doped conducting polymers such as polyaniline present an anionic insertion mechanism which results in detrimental performance for lithium batteries. On the other hand, during the last two decades lithium reversible cells have been under optimization of diverse technologic aspects, making them real viable systems. The introduction of lithium technology resulted in an increase of the specific energy and energy density values vs. the performance of conventional systems as it is shown in figure 1.7. Nevertheless, the use of metallic lithium as anode was still problematic, limiting the possible technologic application [49]. Nowadays, the lithium anode has been substituted by low potential insertion materials such as Li_xC_6 [49]; which is capable of accepting and exchanging large amounts of Lithium. These new systems, where the anode and the cathode are formed by solid phases that intercalate lithium ions at different potentials, have been named lithium ion batteries or rocking chair; and they provide better cyclability and safer performance making them a commercial reality. In 1991, Sony commercialized the first lithium ion battery with a carbon anode and a $LiCoO_2$ cathode, having a potential exceeding 3.6V (3 times that of alkaline systems). The following optimization approach for this lithium ion battery was carried out by replacing the liquid electrolyte by a dry polymer electrolyte. Researchers from Bellcore introduced the polymeric electrolyte onto the liquid Li-ion system, developing the first dependable and practical rechargeable Li-Ion battery called plastic Li ion (PLiON), and giving way to thin-film battery technology. This technology offers shape adaptability, flexibility and lightness. This technology is commercially available since



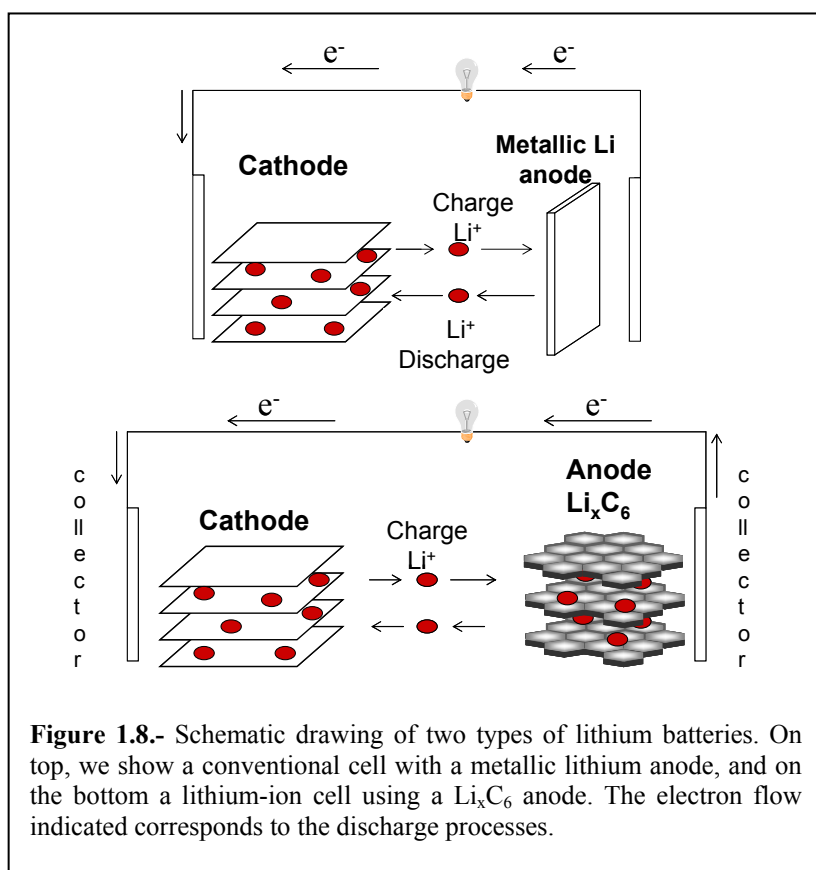
1999 and has many prospective advantages in the continuing trend towards electronic miniaturization. Comparing with mature batteries technologies, such as lead-acid and Ni-Cd, rechargeable Li-based battery technologies are still in their infancy, leaving much hope for future improvement.

1.2.1.2 How does a lithium battery works?

In the first lithium ion cells, as we mention before, metallic lithium was used as the negative electrode and an intercalation compound as the cathode. In this cell, the current is produced because the lithium atoms are oxidized and liberate electrons on the negative electrode giving positive ions (Li^+) that diffuse through the electrolyte. In the positive electrode (cathode) other lithium ions intercalate reversibly to compensate the negative excess charge, resulting from the reduction that takes place in the cathode with the electrons that come from the anode through the external circuit [50]. During the recharge process, a voltage is applied to the cell in a way that the active material on the positive electrode is oxidized (it re-oxidizes losing electrons that were gained during the discharge), and the active material from the negative electrode is reduced (wins electrons that were lost during the discharge). At the same time a

double migration of lithium ions takes place, from the positive electrode to the electrolyte, and from the electrolyte to the negative electrode in order to maintain the charge balance.

For the case where metallic lithium anode is used, it is precisely during the recharge process when the lithium dendrites are



electrodeposited. This problem can be solved using intercalation anodes of lithium, like Li_xC_6 . In figure 1.8 we show the schematic reactions of both types of cells.

1.2.1.3 Lithium insertion electrodes

Lithium battery technologies will highly contribute to our way of life in terms of energy. Nevertheless, the advanced batteries will not be carried out without the support of new or advanced materials. The materials that were used more frequently (as we already mention) as insertion electrodes were the chalcogenides or oxides of transition metals, strongly oxidizing compounds that were capable of reversibly intercalating cations during their reduction and eliminating them during the oxidation. Combined with metallic lithium or lithium insertion anodes (Li_xC_6), (i.e. negative electrodes generating Li^+ during discharge) they lead to “source-sink” processes. Within this wide group of materials, we could mention TiS_2 or WO_3 , or materials based on light transition metals oxides like V_2O_5 or MnO_2 . Vanadium is cheap and easily derived from existing mineral deposits like Mn, and its oxides are attractive cathode materials due to accommodation of three stable oxidation states (V^{+5} , V^{+4} , V^{+3}) within its closely packed oxygen structure. However, V_2O_5 prepared by normal sol-gel methods is still not satisfactory since its capacity fades fast.[51]

More recently, there have been some developments on higher potential systems vs lithium, which were synthesized on their discharge stage. Some examples are LiMn_2O_4 , LiNiO_2 , and LiCoO_2 .

LiCoO_2 is the cathodic material used in commercial batteries. Its cycleability behavior is superior due to its high structural stability (layered structure like $\alpha\text{-NaFeO}_2$ based on a close packed network of oxygen atoms with Li^+ and Co^{3+} ions arranged on alternating (111)planes of the cubic rock salt structure), and can be cycled more than 500 times with 80-90% capacity retention. In addition, its synthesis is easy and has high capacity. [51] The reasons for making an effort on research of new cathode materials are that cobalt is the most expensive component of the battery, and is somewhat toxic. There is a need of cheaper materials before lithium can break through new markets, in particular that of electric vehicles.[52]

LiNiO_2 has a similar layered structure as LiCoO_2 , is far cheaper and has a larger reversible capacity with a high working voltage, but it cannot be utilized unless the serious issue of exothermic oxidation of the organic electrolyte with the collapsing delithiated Li_xNiO_2 structure is solved, which makes the battery unsafe. [43,53]

Another drawback is its preparation difficulty on a large scale with an ideal layered structure, due to the problematic oxidation to Ni^{+3} . [51]

LiMn_2O_4 has a different structure than LiCoO_2 and LiNiO_2 . Since it is cheap, has a high working voltage, high stability of the electrolyte, and has small environmental impact, it is fairly attractive. However, its capacity fades slowly, and this prevents its commercial use. By introducing Ni to this spinel we get a layered structure compound like $\text{LiNi}_{1/2}\text{Mn}_{1/2}\text{O}_2$, which is also very attractive, having a high capacity, high working voltage (3.5-4.0 V vs. Li/Li^+), long cycleability and low price.[51,53]

Recently, research on cathodes based on phosphates of transition metals has resulted in surprising but promising performance.[46] Some examples are iron [46,54] and vanadium [55-57] phosphates that with their redox couples ($\text{Fe}^{3+}/\text{Fe}^{2+}$ and $\text{V}^{4+}/\text{V}^{5+}$) lie at higher potentials than in the oxide form. Some phosphates, sulfates or amorphous hydroxides of Fe are attractive in view of their high-capacity flat working voltage, and low price, though development is still in the early stages. [53] One of the main drawbacks with using these materials is their poor electronic conductivity, which can be enhanced with an intimate contact with carbon [58].

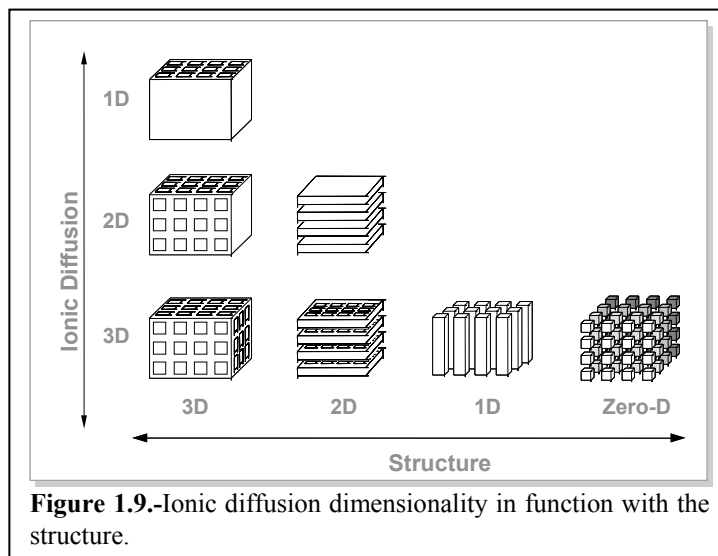
Numerous classes of insertion-deinsertion materials have been synthesized over the last 20 years, but no real gain in capacity has been achieved.[46] The future relies on finding not only the best properties for cathodic materials, but the best-performing combination of electrode-electrolyte-electrode that can be achieved only through the selective use of existing and new materials as negative and positive electrodes, and of the right electrolyte combination; so as to minimize detrimental reactions associated with the electrode- electrolyte interface- the critical phase of any electrochemical system.

Next we will discuss some of the key properties that active cathodic materials are expected to have when used as insertion electrodes for lithium rechargeable batteries. We will focus on ionic conductivity/diffusion, structural reversibility, surface area, and electronic conductivity of the cathodic materials that are precisely the subject of this thesis.

- Ionic conductivity

The insertion and diffusion of ions, is directly related to the host structure and to the presence of vacancies for the ions (in our case Li^+). In principle, we can find

structures that are extended in 1, 2 or 3 dimensions with ionic diffusion paths also with the same dimensions, as in figure 1.9.



In general, the one dimensional structures consist of ribbons joined by weak Van der Waals bonds on the b crystallographic direction (TiS_3 , NbSe_3). The 2D structures consist of layers (VOPO_4 , and several transition metal chalcogenides and dioxides). The 3D structures have interwoven channels permitting the insertion and diffusion of the ion in three directions inside the structure. Obviously, it is necessary that the channel size would be big enough to accommodate the ions. The advantage of 3D structures over 2D ones is that the 3D prevents the intercalation of electrolyte molecules and that the degree of expansion/contraction when lithium is inserted/deinserted is lower [54].

Relating structural dimensionality with the ionic diffusion dimensionality, (figure 1.9) we have examples of 3D structure with 1D ionic diffusion; such as rutile, hollandite and ramsdellite structures. Examples of 2D structures with 2D ionic diffusion are molybdenite phases MX_2 (MoS_2 , TiS_2 and LiNiO_2 , LiCoO_2 , etc.). Among 3D structures with 3D ionic diffusion we have the spinels (LiMn_2O_4). In an extreme case the zero-D open wide structure, represents the ideal ionic diffusion. Nevertheless, this structure cannot be found among extended insertion cathodes since it corresponds to cluster or molecular systems.

- Structural reversibility

Electrochemical charge-discharge is often accompanied by structural changes. The network dimensions are usually a function of the reaction degree and as a consequence, induced tensions arise due to different intercalation gradients throughout the electrode. Fractures appear when the local tension exceeds the matrix elastic limit, and to reduce or liberate this induced mechanical tension, a new phase is formed. In general it is considered that when the lattice unit cell changes more than 15% in any dimension during the insertion or de-insertion reaction, is almost impossible that topotactic reactions occur (reactions with the maintenance or a slight gradual change of the structure); and therefore the reversible structure properties and rechargeability are negatively affected.[59] Solving the problem of structural irreversibility at certain potentials is actually one of the principal objectives in the development of these electrodes; because limits drastically the performance of the system (i.e. specific energy vs. cyclability). [60]

- Surface Area

Turning the morphology or texture of the electrode material to obtain porous and high surface area composite electrodes constitutes another exciting, although less exploited, route to enhance electrode capacities. Tailor made nanostructured materials, such as aerogels, create new opportunities not only at the applied level, but also at the fundamental level where some elementary questions, such as the exact mechanism governing these large capacities remain unanswered.[46]

In this line of work it has been shown that an increase of the specific surface area of the electroactive particles represents an enhancement of the system specific energy. In contrast with this benefit, the electrocatalytic activity of most insertion electrodes give place to detrimental effects, when submitted to high potentials, since the increased surface of the electrode can in turn favor the electrolyte decomposition, losing charge and cyclebility. [54] The challenge is to find the suitable material combination, the maximum compatible voltage avoiding electrolyte decomposition, and/or optimum surface area of the electrodes.

- Electronic conductivity

The low electronic conductivity of most cathodes used in lithium rechargeable cells is normally compensated by conductivity-enhancing additives, typically carbon.

Nevertheless, the disadvantage of using this additive is that affects the specific energy of the system; since it doesn't contribute to the specific charge of the system, and therefore the minimal amount compatible with adequate conductivity should be used.[54]

Summarizing, we can say that the ideal material to be used as cathode on rechargeable lithium cells will be the one that is capable of Li^+ insertion and deinsertion in a reversible way without permanent structural changes, one with high electronic conductivity, with minimal structural barriers for ionic diffusion, with an optimal surface area and inert towards the decomposition of the electrolyte.

Using electroactive oxides can provide ionic conductivity, besides redox characteristics with good structural reversibility. Nevertheless, the application as insertion materials presents some drawbacks derived from i) their poor electronic conductivity and very frequently from ii) structural changes leading to phase transitions that limit the range of Li intercalation and therefore the specific charge. The ideal solutions would involve increasing the electronic conductivity and forming amorphous or quasi amorphous systems, respectively. The integration of oxides within conducting polymer matrices, as presented in this thesis, tackle both of these problems, since the hybrid materials obtained are poorly crystalline and present the combined electroactivity of the oxide and the polymer while the latter contributes both a structural support and electronic conductivity.

1.2.2 Electrochemical Supercapacitors (ESCs)

As it can be seen in Figure 1.5, batteries are great to store relatively large amounts of charge (high energy densities). However, the ionic diffusion processes associated to their working as explained above result in relatively slow processes, which is the reason why batteries score so low in power density in figure 1.7, and why complementary devices related to conventional capacitors are under development.

Batteries are presently being developed with high peak power capability (peak power density as high as 500 to 700 W/kg), but it is not yet known what trade-offs in energy density, cycle life, and cost will result from the need to attain that high power density. Another approach to meeting the high power requirements of the energy storage systems (most notably in electric and hybrid vehicle applications) is to use a pulse power unit in conjunction with the battery. The pulse power unit provides the peak power during accelerations and recovers energy during braking, and the battery

provides the stored energy required to achieve the desired range of the vehicle. The pulse power unit is recharged from the battery during periods when the power demand is less than the average power required by the vehicle. Electrochemical Supercapacitors (ESCs, also often referred to as supercapacitors or ultracapacitors) are promising candidates for the pulse power unit. [61] ESCs fill in the gap between batteries and conventional capacitors. In terms of specific power this gap covers several orders of magnitude.

1.2.2.1 Background

The principle that electrical energy can be stored in a charged capacitor was known since 1745, much before the invention of the first battery by Volta in 1800. The simple electrophysical principle at work was the storage of charge (small amounts of charge) taking place when two metallic electrodes separated by a dielectric material were charged (subject to a difference of potential).

At a voltage difference, V ; established between the plates accommodating charges $+q$ and $-q$, the stored energy, G is [62]

$$G = \frac{1}{2} CV^2 \quad \text{or} \quad G = \frac{1}{2} qV$$

Where G denotes Gibbs free energy. In table I.II we can find a summary of some of the major historical developments related to ESCs.

Table I.II.- History of the Development of the Electrochemical Capacitor. [62]

Year	1957	1969	1975	1978	1984	1990
Development	G.E. Patent	SOHIO Patents	University of Ottawa(funded by Continental Group, Inc.)	NEC/ Matsushita	Pinnacle Research	Matsushita /Isuzu
Construction	Tar-lump black-sulfuric acid electrolyte	Carbon paste-sulfuric acid electrolyte	Mixed oxides ($RuO_2-Ta_2O_5$)	Activated carbon fiber-cloth organic electrolyte	Mixed oxides (based on UO/Continental project)	Activated carbon-aluminum foil organic electrolyte
Market	No market for low-voltage capacitors	No market for low-voltage capacitors	Military	Memory backup	Military, high rate	Ultra-high current power capacitor charge and discharge
Principal energy storage	Double layer	Double layer	Redox pseudo-capacitance	Double layer	Pseudo-capacitance plus double layer	Double layer.

The simple type of capacitor described above was followed by other devices working on a similar charge separation but taking place at a different level. Thus, the new capacitors exploited the charge separation taking place at the double layer formed between an electrode and electrolyte solution. The utilization of this principle to store electrical energy for practical purposes, as in a cell or battery of cells seems to have been first proposed and claimed as an original development in the patent granted to Becker in 1957. The patent described electrical energy storage by means of the charge held in the interfacial double layer at a porous carbon material perfused with an aqueous electrolyte. The principle involved was charging of the capacitance, of the double layer, which arises at all solid/electrolyte interfaces, such as metal, semiconductor, and colloid surfaces.

After Becker, the Sohio Corporation in Cleveland, Ohio, also utilized the double-layer capacitance of high-area carbon materials, but in a nonaqueous solvent containing a dissolved tetraalkylammonium salt electrolyte. Such systems provided higher operating voltages (3.4-4V) owing to the wider electrochemical stability range of nonaqueous electrolytes.

A different principle was used and developed from 1975 to 1981 by Conway [63], based on the concept of pseudocapacitance introduced by D. Craig. In one type of these supercapacitors, energy storage is based on the so-called "pseudocapacitance", C_{ϕ} , associated to the adsorption of H or the electrodeposition of monolayers of some base metals (Pb, Bi, Cu) at Pt or Au. In another type of system, the pseudocapacitance associated with redox oxides was used, typically RuO₂ films in aqueous H₂SO₄ electrolytes working up to 1.4V. This system approaches almost ideal capacitive behavior (see below), with a large degree of reversibility between charge and discharge, and good cycleability over some 10⁵ cycles.

Work on this latter type of systems has been continued by Pinnacle Research Corp. Some military applications have been realized, but the Ru materials required are too expensive for the development of a large-scale capacitor for use in combination with batteries for electric-vehicle motive power. Further developments pursued in this field include the use of solid electrolytes. For instance, an attractive technology using RuO₂ in a thin film in combination with a Nafion membrane, has been developed by Giner Inc. (Waltham, Massachusetts) and gives high specific capacitance. The design avoids a liquid electrolyte and is analogous to membrane electrolyte fuel cell electrodes

The large capacitances (farads per gram) that can be achieved with the RuO₂ film system and also with the carbon double-layer-type capacitors led to the terms “supercapacitor” or “ultracapacitor” being coined for these types of high specific capacitance devices. Recently it has been suggested that the more general term “electrochemical supercapacitors” be used to refer to these systems.

These electrochemical supercapacitors, with characteristics in the twilight between batteries and conventional capacitors, are finding applications in diverse commercial products such as standby power for random access memory (RAM), telephone equipment, as power sources for operating activators, and as elements for long time-constant circuits, etc.

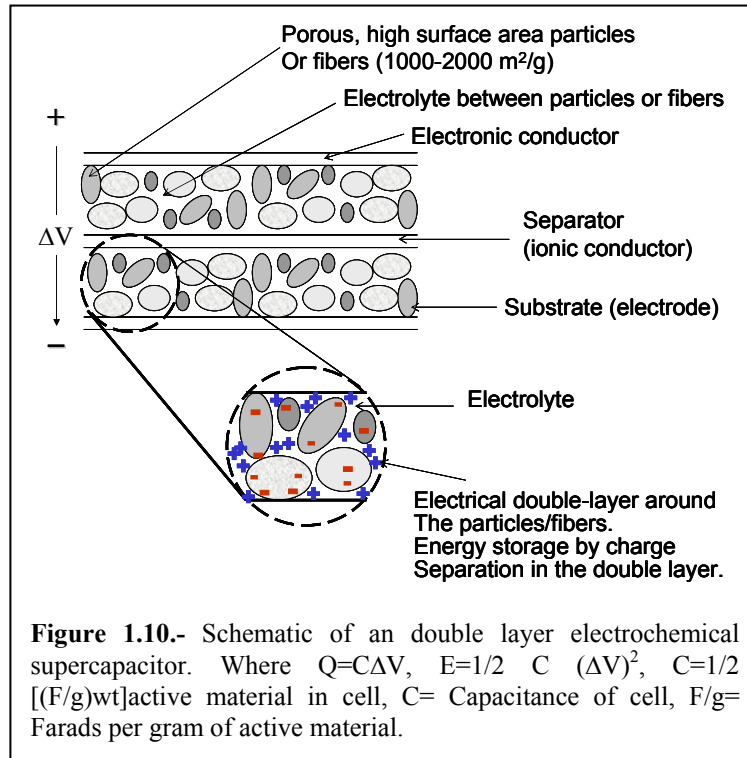
1.2.2.2 How do Electrochemical Supercapacitors work?

Despite the clear distinction made above between double-layer and pseudocapacitance contributions to modern supercapacitors, we should take into account that both mechanisms are normally at work (in different percentages) for a given system and material. Thus, a double layer is also formed between oxide electrodes and electrolytes although in these cases faradaic charge (pseudocapacitance) is dominant. Furthermore, carbonaceous materials can be predominantly double-layer systems but will frequently show some pseudocapacitance (typically between 1-5%).[62]

Taking this into account we will describe here in some more detail the construction and working of both types of supercapacitors. In double layer systems energy is stored by charge separation within the micropores of a very high surface area electrode material (typically carbon). The charge separation is distributed throughout the volume of the electrode material in the double layer formed at the liquid-solid interface between the solid electrode material and the liquid electrolyte with which the electrode is impregnated. As shown in figure 1.10, the internal construction of ESCs is much like that of a battery in that it has two electrodes, a separator, and an electrolyte for ion transfer within the cell. In most cases, the two electrodes in the ESCs cell are identical (unlike in a battery where the electrodes are made of the different materials that form the electrochemical couple of the battery).

In principle, in a double layer capacitor the faradaic current is zero (i.e. no electrochemical reactions). But a more complex situation can arise if some, or most, of the ions that enter the double layer are absorbed into the surface of the electrode

(charge transfer) or are intercalated into the material matrix of the electrode. In this case, the electrode-electrolyte interface can store much more charge than in the simple case of the double layer capacitance, and the additional capacitance is referred to as pseudocapacitance.



1.2.2.3 Electrode Material Technologies and Characteristics.

In the last several years, a number of promising material technologies have been identified for use in the development of high energy density ESCs. Three kinds of electrode materials have been used for ESCs. They are high surface area carbon, metal oxides, and conducting polymers. Table I.III can give us an idea of the characteristics of each of these electrodes materials.

More work has been done using carbons for ESCs than any other material. Carbon has been used in a number of forms: particles, fibers, cloth, foams, and carbon/metal composites). In all cases carbon has been chemically activated at high temperatures to attain high surface areas larger than 2000 m²/g with a well developed micropore structure. The carbon is formed into thin electrodes by a number of processes (pressing with and without heat treatment, mixing with a resin, and

spreading as thin layers, paper making, sintering with metal fibers, sol gel, weaving, and extruding). In general, the aim was to attain a thin electrode with a high carbon density and low resistivity. The energy storage mechanism for carbon electrode is mainly due to the double layer capacitance formed near the carbon surface. Specific capacitances of the electrode as high as 280 and 120 F/g have been measured from activated carbon electrodes in aqueous and nonaqueous electrolytes, respectively.

Table I.III.- Summary of the characteristics of electrode technological materials

ELECTRODE MATERIAL	SPECIF. CAPAC. (F/g)	SURFACE AREA (m²/g)	DENSITY (g/cm³)	RESISTIVITY (Ω-cm)
Carbon/metal composites	100 to 200	1000 to 1500	0.5 to 0.7	<0.01
Aerogel carbon	120 to 160	500 to 800	0.4 to 0.8	<0.01
Doped-polymer (Polyaniline)	400 to 500	200 to 400	0.5 to 0.9	0.01
Anhydrous Ruthenium oxide	100 to 150	100 to 150	2.5 to 3.0	<0.001
Hydrous Ruthenium oxide	600 to 770	80 to 100	2.3 to 2.5	0.002 to 0.005

These values have been taken from ref. [63], but it should be noted that specific values are very dependent both upon the particular materials used and upon cycling conditions, which are not specified.

Maximum voltages of about 0.8 and 3.0 V can be applied to the capacitor made with carbon electrodes when aqueous and nonaqueous electrolytes are used, respectively.[64]

Metal oxides and conducting polymers store energy mainly through redox reaction (or pseudocapacitance). Conducting polymers can be generated by electrochemical and chemical methods. Research on the use of doped polymers as active electrode materials for electrochemical supercapacitors has been in progress since the initial work at the Los Alamos National Laboratory in 1992. A thin, high surface area layer of conducting polymer, such as polyaniline, is electrochemically grown on carbon cloth, or metallic foil current collector, to form the electrode. During the electrochemical formation process, the electrode material can be p-doped or n-doped. When the electrode is charged or discharged, the doping ions move back and forth the polymer into the double layer formed in the micropores of the electrode.

These devices utilize pseudocapacitance rather than simple double-layer charge separation for energy storage. As a result, the specific capacitance of these electrodes is very high (400 to 500 F/g of active material [61] but it should be noted that specific values are very dependent both upon the particular materials used and upon cycling conditions which are not specified).

Three general types of electrochemical supercapacitors can be constructed using conducting polymers as electrode materials. For the type I capacitor, two identical p-doped conducting polymer films are used for both electrodes; in the type II capacitor, two different p-doped conducting polymers are used as active materials on two electrodes; and in the type III capacitor, p- and n-doped conducting polymers are used as active materials on the positive and the negative electrodes, respectively. For the state of the art type I and type II capacitors, the operating voltages is less than 1.0 and 1.5 V, respectively. Because of the low operating voltage range, both aqueous and nonaqueous electrolytes may be used in these kinds of capacitors. For the type III capacitors, the operating voltage can be as high as 3.1 V. Therefore, only the nonaqueous electrolyte can be used in this type of capacitor. [61,64]

Electrochemical supercapacitors using metal oxide materials for the electrodes have been under development for nearly twenty years. Most of the work has been done using ruthenium and tantalum oxides. It is generally accepted that the dominant energy storage mechanism is redox pseudocapacitance. The highest C_p of 380 F/g (150 to 200 $\mu\text{F}/\text{cm}^2$) has been reported for a RuO_2 film with the specific surface area of 120 m^2/g . The maximum voltage range is about 1.4V. The capacitance of this oxide increases by increasing the surface area. It was found that for amorphous phase $\text{RuO}_2 \cdot x\text{H}_2\text{O}$ electrode, fast redox reactions can occur not only at the surface of the electrode but also in the bulk of the electrode. Apparently, the amorphous nature of $\text{RuO}_2 \cdot x\text{H}_2\text{O}$ makes the bulk of the electrode accessible to proton intercalation, increasing its capacitance up to 768 F/g, twice the value than for crystalline RuO_2 films. [64]

As in most electrochemical technology development, the materials requirements are usually of vital importance. For ESCs development, the materials to be used can be chosen according to the end use of the device, but some general requirements applicable to most systems (but substantially different from those for battery electrodes) can be formulated:

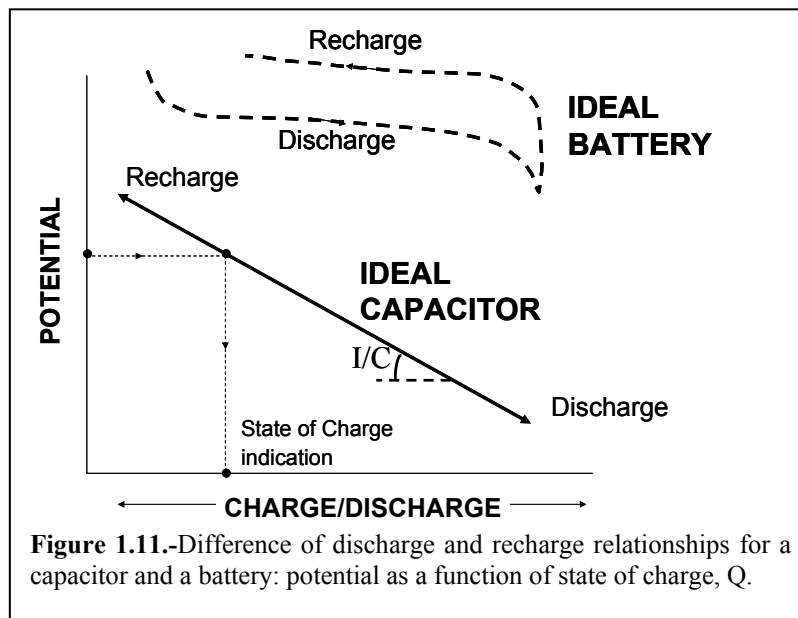
- Capability for multiple cycling, cycle life $>10^5$ cycles;
- Long term stability, related to cycle life;
- Resistance to electrochemical reduction or oxidation of the electrode surface;
- High specific area, on the order of 1000-2000 m^2/g ;
- Maximum operating potential range of cycling within the decomposition limit of the solution (related to resistance to oxidation or reduction);
- Optimized pore size distribution for maximum specific area but minimized internal electrolyte resistance;
- Good wettability, hence favorable electrode/solution interface contact angle (depends on pore structure);
- Minimized ohmic resistance of the actual electrode material and contacts;
- Capability of material being formed into electrode configurations having mechanical integrity (compressed powders with binder, fiber or woven fiber matrices, aerogel materials, glassy carbon structures) and minimum self-discharge on open circuit.

In relation to the above ideal requirements, the active area, or active weight or volume, is a common concept involved in descriptions or specifications of battery electrodes. It refers to the active mass of electrode materials that can undergo the required electrochemical redox reactions of the battery. A similar term can be applied to electrochemical supercapacitors; in the case of double-layer-type capacitors, it refers to the real area of electrode matrices that can undergo electrostatic charge acceptance or charge depletion. In the case of redox-pseudocapacitance devices, the terms have the same significance as for battery systems, but the real accessible electrode area is also usually important because this determines power performance.[40]

1.2.3 Comparison of Electrochemical Supercapacitor and Battery Charging curves.

As pointed out above, the energy associated to the charging of a capacitor to a plate voltage difference of V is $(1/2)CV^2$. It is an electrostatic free energy (Gibbs energy), G . For a battery process, the maximum Gibbs energy is the product of charge Q and the difference of potential, ΔE , between the Nernstian reversible potentials of the two electrodes, $G=Q \cdot \Delta E$. For the capacitor case, for an accommodated charge Q , G is $(1/2)QV$. For a given electrode potential difference, $\Delta E=V$, in the two cases it is

then evident that the energy stored by a two-electrode cell accommodating a given Faradaic charge Q at voltage $\Delta E=V$, is twice that stored in a capacitor charged with the same Q to the same voltage. This difference can be understood in the following way: In the process of charging a pure double-layer capacitor every additional element of charge that is added has to do electrical work (Gibbs energy) against the charge density already accumulated on the plates, progressively increasing the interelectrode potential difference. In a battery cell being charged, a thermodynamic potential (ideally) exists independent of the extent of charge Q added, so long as the two components (reduced and oxidized forms) of the electroactive material remain coexisting. Thus the potential difference of the battery cell is ideally constant throughout the discharge or recharge half-cycles, so that G is $Q \cdot \Delta E$ rather than $Q \cdot 1/2 \Delta E$ (or $1/2V$). This difference can be illustrated by the discharge curves shown schematically in figure 1.11 where the voltage on the capacitor declines linearly with the extent of charge, while that for an ideal battery remains constant as long as two phases remain and are in equilibrium.



The decline of the capacitor voltage arises formally and phenomenologically since $C=Q/V$ or $V=Q/C$; therefore $dV/dQ=1/C$. The ideal battery cell voltages on discharge and recharge, as a function of state of charge are shown as parallel lines of zero slope in the upper parts of the diagram. These two lines differ as a result of any

cathodic and anodic polarization (including so-called ohmic IR potential drop due to internal or solution resistance) arising in the discharge or recharge half-cycles. In the sloping discharge and recharge line for the capacitor (figure 1.11), there will also be significant IR drop, depending on the discharge or recharge rates, that is, the discharge line will actually be somewhat separated from the recharge line by a voltage difference equal to $2IR$.

An important transitional behavior between electrochemical capacitors and batteries arises with processes involving Li^+ intercalation into layered host cathode material. Normally cathode materials, coupled with a Li anode or a Li-C anode, would be regarded as battery cathode materials. However, the forms of the charge and discharge curves and associated pseudocapacitance are similar to those for 2-dimensional electrosorption. This class of materials exhibits properties intermediate between those of bulk-phase battery reagents and quasi-2-dimensional pseudocapacitor electrodes.

Through this introduction we have seen how the fields of conventional rechargeable batteries and conventional capacitors have merged into a general field of energy storage under the label of electrochemical supercapacitors thanks to the development of creative combinations between new materials and devices.

The field of electroactive hybrid materials based on COPs and inorganic redox species that has been developed by our group exemplifies this type of innovative approach towards developing novel energy storage models and is expanded here as part of the present Thesis.

1.3 OBJECTIVES OF THE PRESENT WORK

The general objective of this thesis has been to advance in the knowledge of hybrid materials based on COPs by optimizing certain materials already known, by preparing novel combinations and finally by testing the performance of the materials prepared and characterized in rechargeable lithium batteries and electrochemical supercapacitor cells. In some more detail, our specific objectives can be stated as follows:

- Study of hybrid materials based on inorganic electroactive species (V_2O_5 , MnO_2 , $VOPO_4$, PMo_{12} , SiW_{12} and PW_{12}) and conducting organic polymers (Polyaniline, Polypyrrole),
- Development of new hybrid materials based on non-layered oxides such as manganese oxides (MnO_{2-x}) with polyaniline or polypyrrole. This series of materials was to be prepared by in-situ simultaneous growth of the organic and inorganic phases.
- Optimization of synthetic procedures for the Polyaniline/ V_2O_5 system. This objective aimed at establishing the synthesis reproducibility, determining effects on the microstructure and electrochemical properties, and trying to improve the preparation methods and the performance in Li cells of a hybrid system that had been previously studied in our group.
- Besides the hybrid study, we were also interested in determining the performance of parent inorganic phases (for example V_2O_5 xerogels, for the above mentioned hybrids) in the same energy storage devices. In this particular case we would carry out a comparative analysis of their properties as Li insertion electrode materials.
- Design and synthesis of “triple” hybrid materials. This novel type of hybrids would try to combine the integration of molecular inorganic species into COPs and the insertion of the latter into extended inorganic phases in a single material. In other words it would try to combine both O-I and I-O approaches to lead to materials that we could label as I-O-I.
- Design and synthesis of new hybrid IO hybrid materials based on other layered inorganic phases, such as vanadyl phosphate ($VOPO_4$). Characterization from a structural, chemical and electrochemical point of view. Tests for their possible application as cathodes in rechargeable lithium batteries.
- Exploration of the capabilities of our hybrid materials for novel applications. In particular, assessing the possibility of OI hybrids based on COPs and clusters of PMo_{12} , SiW_{40} and PW_{12} .to shift from Li battery applications towards their use as electrodes for electrochemical capacitors.

In every case the research has been carried out in three fundamental stages: the material synthesis by means of chemical, electrochemical or sol-gel synthetic techniques; the corresponding basic characterization, which includes chemical

analysis, TGA, FTIR, etc; and finally some basic electrochemical characterization, followed by tests for application in specific energy storage devices.

REFERENCES

- [1] Gómez-Romero, P.; *Adv. Mat.* **2001**(13), 163.
- [2] Yacamán, M.J.; Rendón, L.; Arenas, J.; Serra Puche, M.C.; *Science* **1996**(273), 223.
- [3] Judeinstein, P.; Sanchez, C.; *J. Mater. Chem.* **1996**(6), 511.
- [4] Coronado, E.; Palacio, F.; Veciana, J.; *Angew. Chem. Int.Ed.* **2003**(42), 2570.
- [5] Deronzier, A.; Moutet, J.-C.; *Coord. Chem. Rev.* **1996**(147), 339.
- [6] Kulszewicz-Bajer, I.; Zagorska, M.; Pron, A.; Billaud, D.; Ehrhardt, J.J.; *Mater. Res. Bull.* **1991**(26), 163.
- [7] Lapkowski, M.; Bidan, G.; Fournier, M.; *Synth. Met.* **1991**(41-43), 407.
- [8] Gómez-Romero, P.; Lira-Cantú, M.; *Adv. Mat.* **1997**(9), 144.
- [9] Fabre, B.; Bidan, G.; *Electrochim. Acta* **1997**(42), 2587.
- [10] G. Torres-Gómez, G.; Lira-Cantú, M.; Gómez-Romero, P.; *J. New Mater. Electrochem. Syst.* **1999**(2), 145.
- [11] Gómez-Romero, P.; Casañ-Pastor, N.; Lira-Cantú, M.; *Solid State Ionics* **1997**(101-103), 875.
- [12] Fabre, B.; Bidan, G.; *Adv. Maert.* **1993**(5), 646.
- [13] www.mete.mtesz.hu/kiado/oszk/oszk_2002/oszk2002_6/pdf/6_2.pdf
- [14] Hasik, M.; Pron, A.; Kulszewiczbajer, I.; Pozniczek, J.; Bielanski, A.; Piwowarska, Z.; Dziembaj, R.; *Synth. Met.* **1993**(55), 972.
- [15] Hasik, M.; Pron, A.; Pozniczek, J.; Bielanski, A.; Piwowarska, Z.; Kruczala, K.; Dziembaj, R.; *J. Chem. Soc. Faraday Trans.* **1994**(90), 2099.
- [16] Lira-Cantú, M.; Gómez-Romero, P.; *Recent Res. Dev. Phys. Chem.* **1997**(1), 379.
- [17] Lira-Cantú, M.; Gómez-Romero, P.; *Chem. Mater.* **1998**(10), 698.
- [18] Gómez-Romero, P.; Lira-Cantú, M.; *Adv. Mater.* **1997**(9), 144.
- [19] Torres-Gómez, G.; Gómez-Romero, P.; *Synth. Met.* **1998**(98), 95.
- [20] Gangopadhyay, R.; De, A.; *Chem. Mater.* **2000**(12), 608.
- [21] Hu, C.C.; Chen, E.; Lin, J.Y.; *Electrochim. Acta* **2002**(47), 2741.
- [22] Wan, M.; Zhou, W.; Li, J.; *Synth. Met* **1996**(78), 27.
- [23] Kuwabete, S.; Kisimoto, A.; Tanaka, T.; Yoneyama, H.; *J. Electrochem. Soc.* **1994**(141), 10.
- [24] Huang, C.L.; Partch, R.E.; Matijevic, E.; *J. Colloid Interface Sci.* **1955**(170), 275.
- [25] Gebeyehu, D.; Brabec, C.J.; Sariciftci, N.S.; Vangeneugden, D.; Kiebooms, R.; Vanderzande, D.; Kienberger, F.; Schindler, H.; *Synth. Met.* **2002**(125), 279.
- [26] Kim, Y.G.; Walter, J.; Samuelson, L.A.; Kumar, J.; *Nano Lett.* **2003**(3), 523.
- [27] Avvaru, N.R.; Tacconi, N.R.; Rajeshwar, K. *Analyst* **1998**(123), 113.
- [28] Arango, A.C.; Carter, S.A.; Broca, P.J.; *Appl. Phys. Lett.* **1999**(74), 1698.
- [29] Maeda, S.; Armes, S.P.; *Synth. Met.* **1995**(73), 151.
- [30] Nakajima, H.; Matsubayashi, G.E.; *Chem. Lett.* **1993**, 1993.
- [31] De Stefanis, A.; Foglia, S.; Tomlinson, A.G.; *J. Mater. Chem.* **1995**(5), 475.
- [32] Kinomura, N.; Toyama, T.; Kumada, N.; *Solid State Ionics* **1995**(78), 281.
- [33] Ohsawa, T.; Kimura, O.; Kabata, T.; Katagiri, N.; Fuji, T.; Hayashi, Y.; "Polymer Film Battery using New Type Electrode", *Electrochem. Soc. Proc.* **1995**(94-98), 481.
- [34] Wu, C.G.; DeGroot, D.C.; Marcy, H.O.; Schindler, J.I.; Kannewurf, C.R.; Liu, Y.J.; Hirpo, W.; Kanatzidis, M.G.; *Chem. Mater.* **1996**(8), 1992.
- [35] Somani, P.R.; Marimuthu, R.; Mandale, A.B.; *Polymer* **2001**(42), 2991.
- [36] Huguenin, F.; Torresi, R.M.; Buttry, D.A.; *J. Electrochem. Soc.* **2002**(149), A546.
- [37] Oliveira, H.P.; Graeff, C.F.O.; Brunillo, C.A.; Guerra, E.M.; *J. Non-Cryst. Sol.* **2000**(273), 193.
- [38] Goward, G.R.; Leroux, F.; Nazar, L.F.; *Electrochimica Acta* **1998**(43), 1307.
- [39] Demets, G.J.F.; Anaissi, F.J.; Toma, H.E.; *Electrochim. Acta* **2000**(46), 547.
- [40] Kuwabata, S.; Masui, S.; Tomiyori, H.; Yoneyama, H.; *Electrochim. Acta* **2000**(46), 91.

- [41] Kanatzidis, M.G.; Wu, C.G.; Marcy, H.O.; DeGroot, D.C.; Kannewurf, C.R.; *Chem. Mater.* **1990**(2), 222.
- [42] Kwon, Chai-Won; Murugan, A.V.; Campet, G.; Portier, J.; Kale, B.B.; Vijaymohanan, K.; COI, J.H.; *Electrochem. Común.* **2002**(4), 384.
- [43] Edwards, J.H.; Badwal, S.P.S.; Duffy, G.J.; Lasich, J.; Ganakas, G.; *Solid State Ionics* **2002**(152-153), 843.
- [44] Dell, R.M.; Rand, D.A.J.; *J. Power Sources* **2001**(100), 2.
- [45] Kötz, R.; Carlen, M.; *Electrochim. Acta* **2000**(45), 2483.
- [46] Tarrascon, J.M.; Armand, M.; *Nature* **2001**(414), 359.
- [47] Brandt, K.; *Solid State Ionics* **1994**(69), 173.
- [48] Geniés, E.M.; Boyle, A.; Lapkowski, M.; Tsintavis, C.; *Synth. Met.* **1990**(36), 139.
- [49] Scrosati, B.; *Nature* **1995**(373), 173.
- [50] Glanz, J.; *Science* **1994**(264), 1084.
- [51] Wu, Y.P.; Rahm, E.; Holze, R.; *Electrochim. Acta* **2002**(47), 3491.
- [52] Ritchie, A.G.; Giwa, C.O.; Lee, J.C.; Bowles, P.; Gilmour, A.; Allan, J.; Rice, D.A.; Brady, F.; Tsang, S.C.E.; *J. Power Sources* **1999**(80), 98.
- [53] Takamura, T.; *Solid State Ionics* **2002**(152-153), 19.
- [54] Thackeray, M.; *Nature.* **2002**(1), 81.
- [55] Azmi, B.M.; Ishihara, T.; Nishiguchi, H.; Takita, Y.; *Electrochim. Acta* **2002**(48), 165.
- [56] Kerr, T.A.; Gaubicher, J.; Nazar, L.F.; *Electrochem. and Solid State Lett.* **2000**(3), 460.
- [57] Park, N.G.; Kim, K.M.; Chang, S.H.; *Electrochem. Comm.* **2001**(3), 553.
- [58] Huang, H.; Yin, S.C.; Nazar, L.F.; *Electrochem. and Solid State Lett.* **2001**(4), A170.
- [59] Ohzuku, T.; Ueda, A.; *Solid State Ionics* **1994**(69), 201.
- [60] Lira-Cantú, M.; “*Materiales Híbridos Orgánico-Inorgánico a Base de Fosfomolibdato o Pentóxido de Vanadio Dispersos en Polímeros Orgánicos Conductores. Aplicación como Electrodo de Inserción en Baterías de Litio.*” Ed. Universitat Autònoma de Barcelona, Barcelona, **1997**, pp 244.
- [61] Burke, A.F.; Murphy, T.C.; *Mat. Res. Soc. Symp. Proc.* **1995**(393), 375.
- [62] Conway, B.E.; “*Electrochemical Supercapacitors. Scientific Fundamentals and Technological Applications*”, Kluwer Academia/Plenum Publishers, New York, **1999**, pp 698.
- [63] Conway, B.E.; Birss, V.; Wojtowicz, J.; *J. Power Sources* **1997**(66), 1.
- [64] Zheng, J.P.; Huang, J.; Jow, T.R.; *J. Electrochem. Soc.* **1997**(144), 2026.